# GPS, COMMUNICATION AND ENVIRONMENTAL SENSOR BASED COLLISION MITIGATION SYSTEM FOR TRUCKS

**Dipl.-Ing. Marc Wimmershoff**
Institut für Kraftfahrzeuge Aachen (ika), RWTH Aachen University
Germany
**Dipl.-Ing. Stefan Deutschle**
Forschungsgesellschaft Kraftfahrwesen mbH Aachen (fka)
Germany

Paper Number 09-0070

## ABSTRACT

In order to enable state of the art and future accident preventing systems (APS) to react appropriate in traffic situations, it is essential to monitor the driving environment. Therefore a new communication, GPS and environmental sensor based method for APS data acquisition was developed. This method uses GPS, vehicle related driving dynamics data, wireless car-2-car-communication (C2C) and combines them with on-board environmental sensor data (Camera and Lidar sensors).
First a Kalman-Filter based GPS-tracking was developed in order to increase the update rate of GPS. Therefore GPS- and vehicle dynamics data are fused in a dead reckoning system. Second, a Kalman-Filter based 3rd order lane model was implemented using Camera data from ego- and preceding vehicle - transmitted by C2C - for the determination of the relevant target. Beyond vehicle related data are transferred from the target vehicle to the ego-vehicle in order to improve the target selection. The potential of this method was demonstrated in a prototype collision mitigation (CM) system. The system was tested within driving experiments and subsequent simulations with the measured data.
With the new method the accuracy and scope of application of collision mitigation systems can be enhanced, so that the detection and identification of stationary vehicles, for example at the end of traffic jams, is improved. Furthermore a high reliability of the determination of the relevant target for APS can be reached.
As a matter of course the limitation of this approach is the dependency of the system performance (as in all C2C and environmental sensor based systems) on the equipment rate. On the other hand it can be expected that equipment rates will increase in future.

## INTRODUCTION

Regarding commercial vehicles, rear-end collisions count among the most frequent occurring accident types [1]. Especially rear-end collisions with high relative velocities are dangerous if commercial vehicles are involved because of their high mass. The GIDAS data base (**G**erman **i**n-**D**epth **A**ccident **S**tudy) shows that car drivers perform an emergency stop (6 m/s² to 10 m/s²) only in 22 % of all accidents. In approximately 78 % of the collisions an insufficient deceleration (0 m/s² to 6 m/s²) is executed [2]. [3] points out that nearly 60 % of all rear-end collisions and almost one third of all head-on collisions - the correct reaction assumed - could be avoided, if the driver would react half a second earlier. These values show the potential of advanced driver assistance systems (ADAS) supporting the vehicle longitudinal dynamics.
Nowadays, there are already brake assists in series production, initiating an emergency stop, if a collision with a vehicle driving in front seems unavoidable. Further systems are under development. Today, Radar and Lidar sensors as well as Camera systems are the basis for the detection of an imminent collision. Out of this an abundance of challenges arise, for example the recognition of an object standing still or the misinterpretation of warning beacons at motorway constsruction sites. Present series systems only react on moving objects or objects, which were in motion at the beginning of the detection. Within this paper an approach is described that uses the GPS position and further data of the preceding vehicle, all transmitted by C2C to allow a detection of stationary target objects.
This paper is structured as follows: first the Kalman-Filter based models are introduced. On the one hand an Extended Kalman-Filter (EKF) based ve-

hicle model (GPS-Tracking) calculating global positioning data between two GPS data updates is implemented. With the help of this GPS-Tracking and a C2C a position measurement is employed. On the other hand a Kalman-Filter based street model is implemented that uses data measured by ego- and preceding vehicle. The street data from the preceding vehicle is also transmitted by C2C. The next chapter deals with the used hardware. It contains the description of the test vehicles, sensors, C2C, GPS receiver and the utilised computation hardware. Afterwards an overview of the system architecture is given. In the last chapter the results of test drives in real traffic, on the test track and the results of simulations with measured data are presented.

## KALMAN-FILTER BASED VEHICLE- AND STREET MODELLING

The vehicle- and the street model describe the current condition of the vehicle and the environment. The state estimation of the model is supported by a Kalman-Filter.

In a first step a vehicle model is developed, which describes the dynamic movement of the vehicle in Gauß-Krüger (GK) coordinates. In a second step the road is modelled, in order to describe the movements of the host vehicle in the lane and generate a path prediction. Both models are based on state space description. In the following the models and their mathematical formulation are presented.

### Vehicle Model (GPS-Tracking)

The vehicle model describes the position and direction of motion (course) of the vehicle in GK coordinates. Therefore a mass point, moving in the GK coordinate system, is considered (Figure 1). With the GPS data and the subsequent GK coordinate transformation, the x- and y-coordinates of the vehicle ($x_{GK}$ and $y_{GK}$ in Figure 1) are described with the GPS update frequency of 1 Hz. Furthermore, the course angle $\tau$ is given, which is also included in the GPS data. If a speed of 80 kph is assumed for commercial vehicles on motorways, then the vehicle travels 22,22 m within the GPS update rate. Since a GPS based positioning system should be realised, it is necessary to have a higher positioning update of the host vehicle (> 1 Hz). This is realised in an EKF based vehicle model, delivering additional position information between two GPS measurements.

As shown in Figure 1, the course angle $\tau$ has a value of 0° if the vehicle moves into north direction. Furthermore, the positive rotation direction of $\tau$ is clockwise while the positive rotation direction of the vehicle yaw rate $\dot{\psi}$ is counterclockwise. Beyond the yaw angle $\psi_{GPS}$ is defined to be the angle between the y-coordinate of the GK coordinate system and the vehicle's longitudinal central axis.

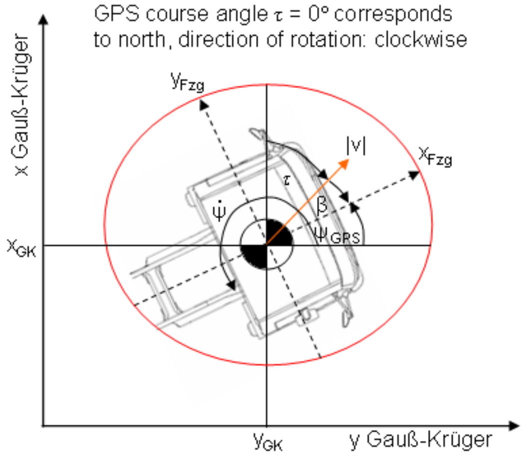


**Figure 1. Angles in GK coordinate system.**

Modelling the mass point's motion in the GK coordinate system can be done on different complexity levels. Within the object modelling two different models are commonly used, the model of constant acceleration or the model of constant velocity.

The model of constant acceleration takes the position, the velocity and the acceleration of the vehicle into account, see Equation (1).

$$p_{k+1} = p_k + v_k \cdot \Delta t + a_k \cdot \frac{\Delta t^2}{2} \qquad (1).$$

The model of constant velocity is a simplification of the model of constant acceleration by leaving out the acceleration term. Thus, Equation (1) is simplifyed to Equation (2).

$$p_{k+1} = p_k + v_k \cdot \Delta t \qquad (2).$$

The movement of the object is described separately in longitudinal- and in lateral direction. Independently which object model is choosed, the state vector **x** for the vehicle model is given by:

$$\mathbf{x} = \begin{bmatrix} x_{GK} & y_{GK} & \psi_{GPS} \end{bmatrix}^T \qquad (3).$$

It includes the position of the vehicle in x- and y-direction in the GK coordinate system and the yaw angel $\psi_{GPS}$. In this paper, the model of constant velocity was chosen as the motion of commercial vehicles (especially on highways) is very steady. For future works the implementation of a constant acceleration model in combination with a multiple model adaptive estimator (MMAE) is planned.

With the model of constant velocity, the discrete model equations for the Kalman filter can be determined. Under consideration of the slip angle β and $v_k \cdot \Delta t$ replaced with $\Delta x_k$ Equation (4) is valid.

$$\begin{bmatrix} x_{GK,k+1} \\ y_{GK,k+1} \\ \psi_{GPS,k+1} \end{bmatrix} = \begin{bmatrix} x_{GK,k} \\ y_{GK,k} \\ \psi_{GPS,k} \end{bmatrix} + \begin{bmatrix} \Delta x_k \cos\beta_k \sin\psi_{GPS,k} + \Delta x_k \sin\beta_k \cos\psi_{GPS,k} \\ \Delta x_k \cos\beta_k \cos\psi_{GPS,k} + \Delta x_k \sin\beta_k \sin\psi_{GPS,k} \\ \dot{\psi}_k \Delta t \end{bmatrix} \quad (4)$$

A visualisation of the state equations is given in Figure 2. Because of the included trigonometric functions, an extended Kalman-Filter must be used.

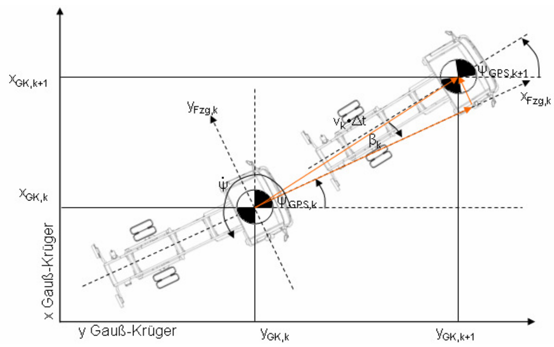


**Figure 2. GPS vehicle motion model.**

The measurement vector **y** is equal to the state vector. Hence the measurement matrix **C** for the vehicle model is given by a 3x3 identity matrix.

## Street Model

For a better understanding the variables used within the street model are introduced according to Figure 3. These are the lateral position of the vehicle in lane ($y_0$) related to the centre of the lane and the relative yaw angle $\psi_{lane}$, showing the orientation of the vehicle in the lane, see Figure 3.

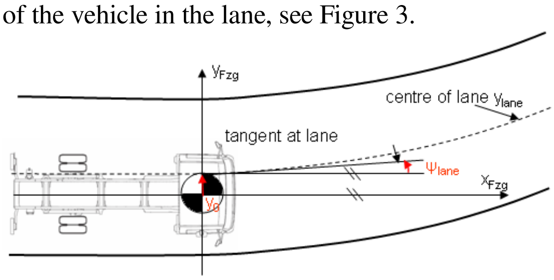


**Figure 3. Lane model and variables [4].**

Generally, the trajectory of the street can be composed of several routing segments, describing a sequence of straight and curved parts. Since the transition from a straight part into a curve with constant radius would mean a sudden step in the road curvature, the transition elements of roads are build as clothoids [5].

**Modelling** – The street model uses a 3rd order polynom according to [4]:

$$y_{lane}(x_{Fzg}) = y_0 + \psi_{lane} x_{Fzg} + \frac{C_o}{2} x_{Fzg}^2 + \frac{C_1}{6} x_{Fzg}^3 \quad (5).$$

This equation describes the trajectory of the lane as a function of the vehicle longitudinal axis. Based on the parameters, needed for the trajectory estimation, the state vector can be derived. Doing so, the lane offset $y_0$, the orientation of the vehicle $\psi_{lane}$, the curvature $C_0$, the change of curvature $C_1$ and the lane width B are state variables of the model.

$$\mathbf{x} = [y_0 \quad \psi_{lane} \quad C_0 \quad C_1 \quad B]^T \quad (6).$$

Using discrete time steps $t_k$ for the lane offset $y_{0,k}$, Figure 4 shows that the following equation is valid:

$$y_{0,k+1} + \Delta y_{Fzg,k} = y_{0,k} + \Delta y_{lane,k} \quad (7).$$

The lane offset of the next time step $y_{0,k+1}$ is thus calculated by the sum of the current lateral lane offset $y_{0,k}$ and the change of the y-coordinate due to the lane curvature ($\Delta y_{lane,k}$), minus the change of the y-coordinate due to yaw movement ($\Delta y_{Fzg,k}$):

$$\Delta y_{lane,k} = \psi_{lane,k} v_k \Delta t + \frac{C_{o,k}}{2}(v_k \Delta t)^2 + \frac{C_{1,k}}{6}(v_k \Delta t)^3 \quad (8).$$

$$\Delta y_{Fzg,k} = v_k \Delta t \sin(\dot{\psi}_k \Delta t) \approx v_k \dot{\psi}_k \Delta t^2 \quad (9).$$

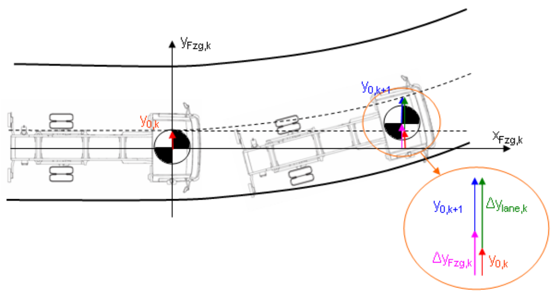


**Figure 4. Lateral position in lane.**

Comparable to the lateral position in lane the angle $\psi_{lane,k+1}$ can be calculated from the sum of $\psi_{lane,k}$ and the change of the angle $\Delta\psi_{lane,k}$ minus the vehicle motion $\Delta\psi_{Fzg,k}$.

$$\psi_{lane,k+1} + \Delta\psi_{Fzg,k} = \psi_{lane,k} + \Delta\psi_{lane,k} \quad (10).$$

$\Delta\psi_{lane,k}$ is equal to the gradient angle of the road at the position $x_{Fzg,k} = v_k \cdot \Delta t$. The gradient angle of a straight line is defined as follows:

$$\alpha = \arctan\left(\frac{\Delta y}{\Delta x}\right) \approx \frac{\Delta y}{\Delta x} = \frac{dy(x)}{dx} \qquad (11).$$

Using a small angle approximation (tan $\alpha \approx \alpha$) it is possible to replace the gradient angle $\alpha$ by the gradient value of the straight line. Transferred to the course of the road (no consideration of the ego-lane angle is necessary), the angle $\Delta\psi_{lane,k}$ is equal to the first derivation of the lane equation (5).

$$\Delta\psi_{lane,k} \approx C_{o,k} v_k \cdot \Delta t + \frac{C_{1,k}}{2}\left(v_k \cdot \Delta t\right)^2 \qquad (12).$$

Furthermore, the yaw angle during the timeframe $\Delta t$ ($\Delta\psi_{Fzg,k}$), can be expressed as follows:

$$\Delta\psi_{Fzg,k} = \dot{\psi}_k \cdot \Delta t \qquad (13).$$

In order to discretise the current curvature $C_0$, the second derivation of (5) respectively the third derivation for the change of curvature $C_1$ can be used.

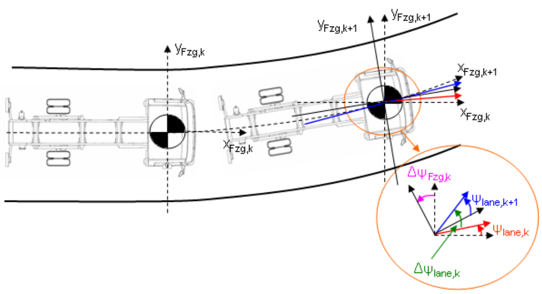

**Figure 5. Relative yaw angle in lane.**

By using discrete points of time for observation, the matrixes needed for the Kalman-Filter are gained with the help of the equations mentioned above. For a better reading the term $v_k \cdot \Delta t$ is substituted by $\Delta x$. Thus, the system matrix **A** is given as follows:

$$\mathbf{A} = \begin{bmatrix} 1 & \Delta x & \Delta x^2/2 & \Delta x^3/6 & 0 \\ 0 & 1 & \Delta x & \Delta x^2/2 & 0 \\ 0 & 0 & 1 & \Delta x & 0 \\ 0 & 0 & 0 & 1 & 0 \\ 0 & 0 & 0 & 0 & 1 \end{bmatrix} \qquad (14).$$

The input matrix **B** takes the yaw rate $\dot{\psi}_k$ and the velocity $v_k$ of the vehicle into account.

$$\mathbf{B} = \left[-v_k \cdot \dot{\psi}_k \cdot \Delta t^2 \quad -\dot{\psi}_k \cdot \Delta t \quad 0 \quad 0 \quad 0\right]^T \qquad (15).$$

The measurement matrix **C** has to be adapted individually to the sensor and the communication.

## USED HARDWARE

Having described the development of the vehicle model and the street model in the previous section, this chapter deals with the used hardware.

For the development and testing of commercial vehicle ADAS, two experimental trucks are available at ika (Institut für Kraftfahrzeuge, RWTH Aachen University). One is an IVECO Stralis AS 440 S 48 T/P EURO 3 with a 16-speed automatic gearbox (Figure 6). The second truck is an IVECO Stralis AS 440 S 48 T/P EURO 5 anticipo with a 12-speed automatic gearbox. Both vehicles are equipped with 367 kW engines, hydrodynamic retarder and WABCO Adaptive Cruise Control. The vehicles' steering is automated with ZF ServoTwin Steering Actuators (torque super position) and the longitudinal dynamic is automated with a WABCO acceleration interface. Thus an external steering and acceleration/braking via CAN bus enabled.

Figure 6 shows one IVECO test truck with the used environmental sensors: a monocular HELLA Camera and HELLA IDIS Lidar sensor. The Camera system is equiped with an algorithm for lane- and vehicle detection and delivers data about surrounding vehicles and the trajectory of the road. The road trajectory data are curvature $C_{0,CAM}$, lane width $B_{CAM}$ and lateral lane offset $y_{0,CAM}$ (compare Figure 7). Beyond, the truck is equipped with a DENSO lane recognition camera, a 77 GHz WABCO Radar sensor and two 24 GHz HELLA Radar Near Distance Sensors (NDS).

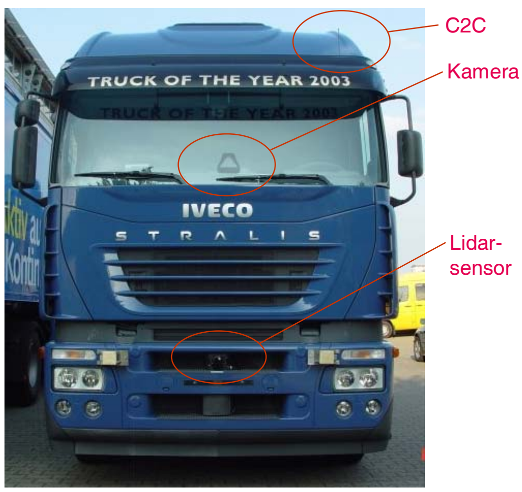


**Figure 6. One of ika's experimental trucks.**

In order to enable a wireless communication between the two trucks, WIRELESS CAN boxes (called WCAN) by Agilion are installed in the trucks. The WCAN boxes allow a wireless connection between two or more network participants and are based on the robust radio technology nanoNET, a wide band communication technology in the 5.8 GHz band.

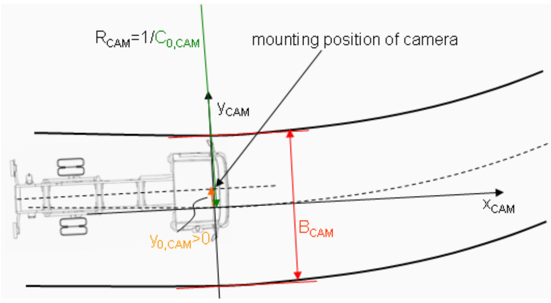


**Figure 7. Data delivered from HELLA camera.**

The GPS receivers used in this work are the GNS 5843 receiver from GNS, Global Navigation Systems company. GNS 5843 is a GPS-RDS/TMC-receiver with a Sirf-III chipset, supporting the NMEA 0183 data protocol. The cycle time is one second.

The target hardware for the developed system is the dSPACE Autobox for rapid prototyping experiments which offers the possibility of testing real-time software on-bord. The software is developed with Matlab/Simulink and compiled with Real Time Workshop for the Autobox.

## SYSTEM ARCHITECTURE

Our communication and environmental sensor based CM system for trucks needs robust data from the ego-vehicle and the environment. Therefore it is necessary to employ a GPS-tracking, that calculates the current position of the vehicle in the GK coordinates. By means of the wireless communication, the GK coordinates and other vehicle relevant signals of a preceding vehicle are received in the following vehile. In combination with the IDIS Lidar sensor data, the received wireless data is combined and delivers a relevant target. Furthermore, the trajectory of the lane is predicted and is available for the CM system.

In the following, the system architecture and modules are described.

**Architecture** – Figure 8 shows the architecture of the system. The measurement data are either used for determinatoin of the relevant target or delivered to the vehicle- or street model.

GPS and vehicle sensors deliver measurement data to the vehicle model, executed each 10 ms. By means of an EKF, a GPS-tracking is built, providing position data of the vehicle in GK coordinates.

The Camera system and the vehicle sensors deliver measurement data to the Kalman-Filter based street model and a robust prediction of the lane trajectory is reached. The street model is triggered with camera measurement data (cycle time 50 ms).

With the help of the IDIS Lidar sensor and the data gained by C2C, the relevant target vehicle is determined. A relevant target can only be present, if the target vehicle and the ego-vehicle drive in the same lane. In this case, the lane trajectory runs through the target vehicle and a correction of the lane trajectory with the help of the relative coordinates of the target vehicle can be performed.

The architecture shown in Figure 8 is for implementation divided into five modules: the GPS modul, WLAN modul, vehicle data model, environmental modul and CM modul.

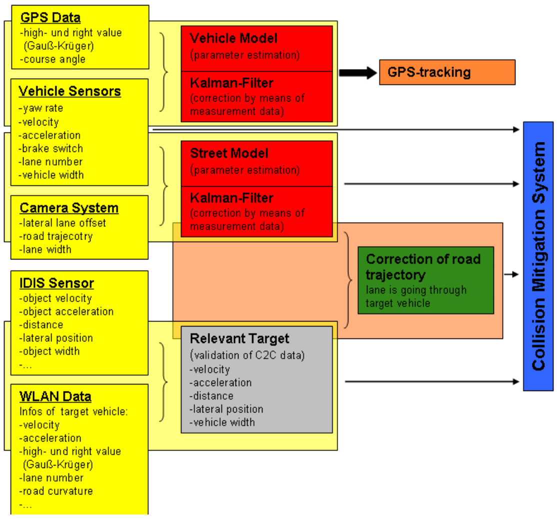


**Figure 8. CM system architecture.**

The GPS modul constains the vehicle model with GPS-tracking while the WLAN modul contains the transmission and receiving of the wireless messages. The vehicle modul is responsible to deliver the vehicle relevant data from CAN bus. The environmental modul contains the algorithm for the determination of the relevant target and the street model. The CM modul consists of the CM system.

**Vehicle Data Modul** – The vehicle data modul delivers the relevant vehicle data from CAN bus and provides these data for further processing. In detail, these data are the yaw rate $\dot{\psi}_{ego}$, the vehicle velocity $v_{ego}$ and the brake switch flag. The vehicle acceleration in longitudinal direction $a_{ego}$ is gained from the velocity by a Luenberger observer [6].

Further signals, generated within the vehicle data modul, are the vehicle width and the lane number. The vehicle width is hard coded with the width of the test vehicle (2.55 m). The lane number is defined as shown on Figure 9.

Up to now, no algorithm for the lane number determination is implemented, thus the lane number for the performed tests was also hard coded.

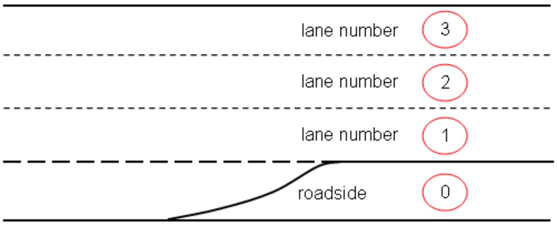


**Figure 9. Definition of lane numbers.**

**GPS Modul** – The GPS Modul contains the GPS-tracking. The GPS-tracking first transforms the GPS position (latitude, longitude and height) into the GK coordinates followed by generation of the measurement vector $\mathbf{y}_{GPS}$. The course angle $\tau$ has to be converted (16). Up to now, the slip angle $\beta$ is not used in the test vehicle, but as the CM system is designed for highways the slip angle can be neglegted and (16) is simplified to (17):

$$\psi_{GPS} = 90° - \tau - \beta \qquad (16).$$

$$\psi_{GPS} \approx 90° - \tau \qquad (17).$$

Hence, the state equations of the vehicle model are:

$$\begin{bmatrix} x_{GK,k+1} \\ y_{GK,k+1} \\ \psi_{GPS,k+1} \end{bmatrix} \approx \begin{bmatrix} x_{GK,k} \\ y_{GK,k} \\ \psi_{GPS,k} \end{bmatrix} + \begin{bmatrix} \Delta x \cdot \sin\psi_{GPS,k} \\ \Delta x \cdot \cos\psi_{GPS,k} \\ \Delta t \cdot \dot{\psi}_k \end{bmatrix} \qquad (18).$$

The measurement vector can be written with the current GK coordinates respectively the yaw angle and is available for the vehicle model.
The input data of the GPS-tracking are the yaw rate and the velocity of the vehicle. For the EKF, the state equations are differentiated with respect to the state vector **x** to obtain the matrix **A**:

$$\mathbf{A} = \begin{bmatrix} 1 & 0 & \Delta x \cdot \cos\psi_{GPS,k} \\ 0 & 1 & -\Delta x \cdot \sin\psi_{GPS,k} \\ 0 & 0 & 1 \end{bmatrix} \qquad (19).$$

Since an GPS update (cycle time 1 s) occurs not in each time step of the vehicle model (cycle time 10 ms), the innovation of the EKF is set to zero, if no GPS update occurred. In this case the state variables of the vehicle model are updated only based on the model itself.

**WLAN Modul** – The WLAN modul receives and transmits data via C2C. The modul of the target vehicle transmits the relevant data while the modul of the ego-vehicle receives data. Transferred data are: velocity, longitudinal acceleration, yaw rate, brake switch, lane number, vehicle width, GK coordinates, lateral position in lane and curvature.
Velocity, longitudinal acceleration, yaw rate, brake switch, lane number and vehicle width are taken from the vehicle data modul while the lateral position in lane and the road curvature are obtained by the environmental modul. The GK coordinates are converted to the coordinates of the truck's rear end. By means of the GK positioning data of the target vehicle's rear and the ego GK positioning data, the relative location of the target vehicle with respect to the ego-vehicle can be calculated, see Figure 10. Therefore, the angle $\alpha_{target}$ is determined:

$$\alpha_{target} = \arctan\left(\frac{x_{GK,target} - x_{GK,ego}}{y_{GK,target} - y_{GK,ego}}\right) - \psi_{GPS,ego} \qquad (20).$$

With the help of $\alpha_{target}$ the relative position of the target vehicle $dx_{GPS}$ und $dy_{GPS}$ can be calculated:

$$dx_{GPS} = \sqrt{(x_{GK,target} - x_{GK,ego}) + (y_{GK,target} - y_{GK,ego})} \cdot \cos\alpha_{target} \qquad (21).$$

$$dy_{GPS} = \sqrt{(x_{GK,target} - x_{GK,ego}) + (y_{GK,target} - y_{GK,ego})} \cdot \sin\alpha_{target} \qquad (22).$$

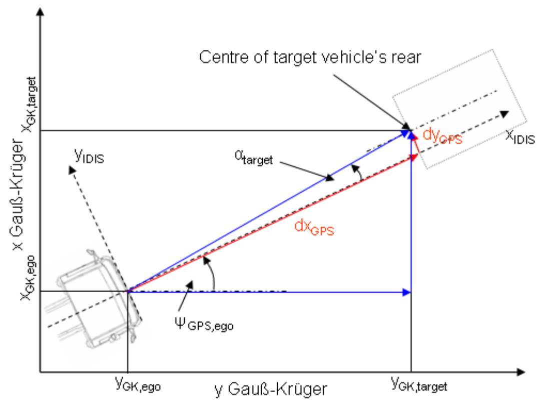


**Figure 10. Determination of the target vehicle's relative position.**

**Environmental Modul** – The environmental modul differs for the ego- and target vehicle. The target vehicle modul consists only of camera data input to transmit them to the ego-vehicle via C2C.
The environmental modul of the ego-vehicle contains the input of the camera data, the input of the IDIS Lidar sensor and an algorithm comparing the IDIS data with the positioning data gained by C2C. Furthermore, the street model is implemented in the environmental modul.
The determination of potential target vehicles consist of the evaluation of the following attributes:

- Object data declared as valid by the sensor
- Distance is less than 100 m
- Object width less than lane width

Furthermore, each IDIS object has a lifetime counter. Having checked these attributes, a list of potential target vehicles is available. The next step for the determination of the target vehicle is depicted in Figure 11. Here, the redundant object data (from C2C and IDIS sensor) are compared. These are the relative object position in x- and y-direction, the velocity, width and acceleration of the target vehicle. For all potential target vehicles the absolute signal difference from IDIS- and C2C data are calculated. For the differences thresholds are defined within the algorithm. If any signal difference is higher than the threshold, the IDIS object is not regarded as target vehicle.

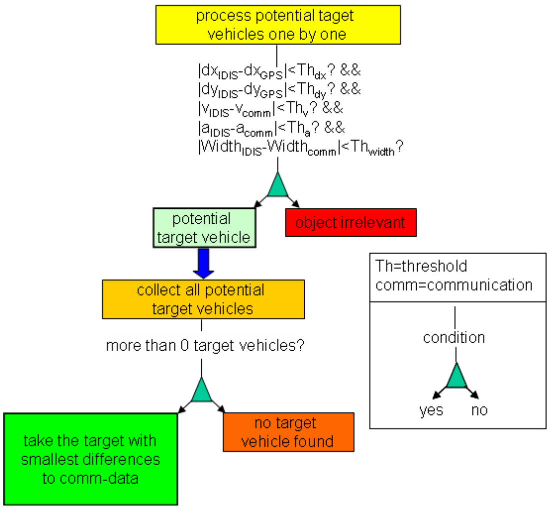


**Figure 11. Determination of target vehicle.**

In case of having more than one IDIS object after this procedure, the algorithm regards that object to be the target vehicle, whose sum of all signal differences is smallest.

The implementation of the street model is also part of the environmental modul in the ego-vehicle. The input signals are the data measured by the camera in the ego-vehicle and the curvature measured by the Camera of the target vehicle, transmitted to the ego vehicle ($C_{0,CAM,target}$). With the knowledge of $C_{0,CAM,target}$ the change of roard curvature is:

$$C_1 = \frac{C_{0,target} - C_{0,ego}}{dx_{target}} \qquad (23).$$

The value $dx_{target}$ describes the distance of the target vehicle in longitudinal direction. The measurement vector $\mathbf{y}_{lane}$ of the street model is now given by:

$$\mathbf{y}_{lane} = [y_{0,CAM,ego} \; C_{0,CAM,ego} \; C_{0,CAM,target} \; B_{CAM,ego}]^T \qquad (24).$$

The output of the Kalman-Filter is the state vector. This signal passes a further function that corrects the state variables $C_{0,ego}$ and $C_{1,ego}$ in case of an existing target vehicle. Is this the case, it is ensured that the ego- and target vehicle drive in the same lane. With the knowledge of the lateral lane offset $y_{0,CAM,target}$ and the position of the target vehicle ($dx_{target}$, $dy_{target}$) the curvature $C^{*}_{0,ego}$ can be calculated by neglecting the change of curvature $C_1$:

$$dy_{target} - y_{0,CAM,target} = y_{0,ego} + \psi_{lane,ego} dx_{target} + \frac{C_{o,ego}}{2} dx_{target}^2 + \frac{C_1}{6} dx_{target}^3 \qquad (25).$$

$$C^{*}_{o,ego} = \frac{2\left(dy_{target} - y_{0,CAM,target} - y_{0,ego} - \psi_{lane,ego} \cdot dx_{target}\right)}{dx_{target}^2} \qquad (26).$$

## EXPERIMENTS AND RESULTS

The developed models are tested in different test drives. While driving, measurement data of the sensors, communication and model data are recorded in the ego-vehicle. The recorded data are later used as input for simulations in Matlab/Simulink. Thus, the model parameter can be modified and the effect can be evaluated.

For tuning of the GPS-tracking, test drives without target vehicle are executed. In order to examine the functionality of the street model and to give a statement about the C2C and GPS based position measurement accuracy, test drives with two test vehicles are executed. The test drives are carried out at different velocities on straight and curved roads and on a test track with a static target vehicle and the ego-vehicle approaching at different velocities.

### Function check and tuning of GPS-tracking

The first manoeuvre for the function check of the GPS-tracking is a steady-state circle drive. Six tests are carried out, clockwise and three counterclockwise on a diameter of 80 m and 40 m. The tests on the 80 m diameter are done with a velocity of 25 kph and 40 kph while the tests on the 40 m diameter are done with 25 kph. An evaluation of a test on the 80 m circle with 25 kph before and after filter tuning is depicted in Figure 12.

In the lower diagram of Figure 12 it can be seen that the model behaviour after the filter tuning delivers better results. The evaluation of the test drive delivers a diameter of 80.35 m (corresponds to a difference of 0.35 m). If all tests are taken into account, the maximum difference for the 80 m circle is 2.5 m and for the 40 m circle 2 m.

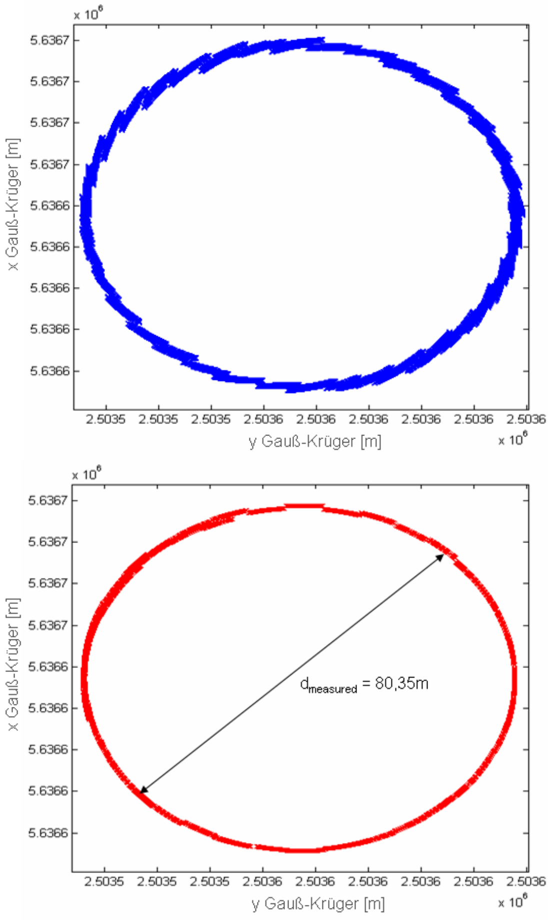


**Figure 12. Results of GPS-tracking before (above) and after filter tuning (below).**

Despite the filter tuning the circle in the lower diagram of Figure 12 shows steps in the signal due to GPS data update. Between two GPS data updates the GK coordinates and the course angle are updated model based. The evaluation of the tests with tuned filter parameters shows that the maximum difference between the new received GPS position and the model based position is less than 1.5 m. Thus, it can be stated that the vehicle model delivers valid data. To ensure that the vehicle model delivers not only in steady-state scenarios valid data, test drives in real traffic are executed.

Here the GPS- and vehicle data were also recorded for later offline simulations and the result is shown in Figure 13.

The track contains straight parts and also curves with large and small radii. Hence, it is well used to examine the model function and perform a filter tuning. In Figure 13 red and blue position plots are given. The blue plots show the GPS measurement data from the receivers. The red plots are the tracked coordinates after further filter tuning.

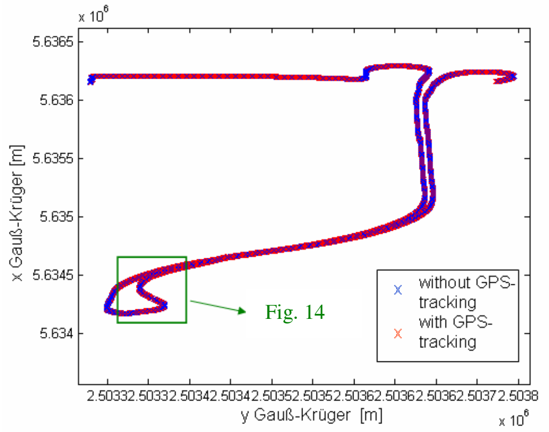


**Figure 13. Measurement on real road.**

Figure 14 shows a detail from the track (green in Figure 13). The model is doing well on straight and curved parts with a slight tendency to less accuracy for increasing curvature. The course angle $\tau$ is on the one hand less accurate during a change of motion direction and on the other hand time-delayed. Furthermore, the side slip angle $\beta$ is neglected, which is correct for highway driving conditions but leads to mistakes on narrow curves. Hence, using a receiver with a better course angle and implementing a slip angle estimator could increase the results.

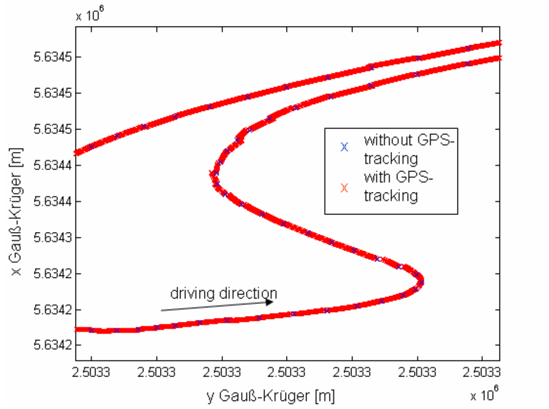


**Figure 14. Extract of measurement.**

As a further factor the traction and brake slip influences the performance. During strong acceleration and deceleration a higher difference between new measured and estimated position was found. In order to remove this influence, a reference velocity should be used in future, weighting the front axle speed sensors more during acceleration and rear axle speed sensors more during deceleration. Within all tests the largest difference between measured and estimated position was 2.51 m with an average value of 0.57 m after filter tuning.

## Function check and tuning of street model

Comparable to the functional check of the vehicle model, driving tests were performed for testing and filter tuning of the street model.

In total 30 test runs were done for the functional check, ⅓ on straight roads, ⅓ on positive curvature (left turn) and ⅓ on negative curvature (right turn), with velocities between 60 to 90 kph. For the later offline simulations and tuning of the street model, again all relevant data were recorderd. Tuning of the object plausibility check algorithm is described in a later section, the simulation results of the street model are described now.

Figure 15 shows the lateral position in lane for a test drive on a straight road. The measurement data are marked blue and the model data red.

At the beginning, the Kalman-Filter needs some time to engage (Figure 15). Regarding the measured position in lane, at 12 s one can see a dropout. The sensor system did not detect the lane correctly, but the street model delivers a steady signal and is not influenced by this dropout.

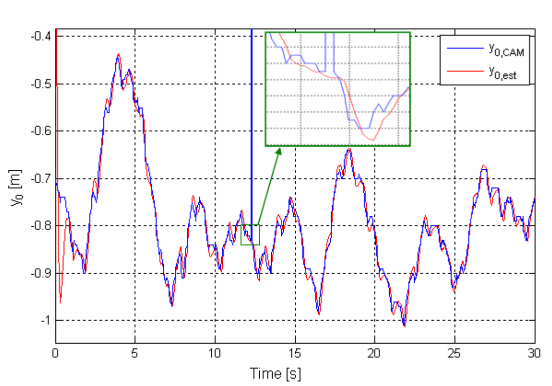


**Figure 15. Measured and estimated position.**

Figure 16 shows the results for the lane width of the same run. Here one can also find the dropout in the blue measurement data at 12 s and again the model based red signal is stable and not influenced. The lane width delivers correct values between 3.6 and 3.8 m which are in the range of values defined for German highways (3.75 m according to [5]).

In order to give a statement about the quality of the curvature and curvature change signal, the tests on curved roads are used. The test track is the last part of the highway A544 in Aachen, shown in Figure 17 (marked blue). The test track is driven in both directions in order to get data of right-hand- (negative curvature) and left-hand bend (positive curvature). With the help of a satellite picture and GPS data, a reference value for the radius of this curve was determined to 600 m (curvature 0.00167 $m^{-1}$).

The test drives were done with 60 and 90 kph and different distances (varying from 15 to 100 m) between the trucks in order to evaluate distance influences on the result.

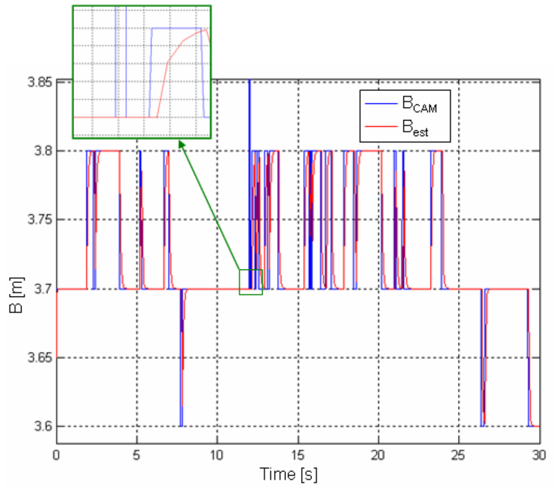


**Figure 16. Measured and estimated lane width.**

The evaluation of one measurement is shown in Figure 18. Because of the driving direction, positive curvature values should occur (direction 2, see Figure 17). Again the measurement data are marked blue, model data are marked red and the filter needs some time to engage on the beginning.

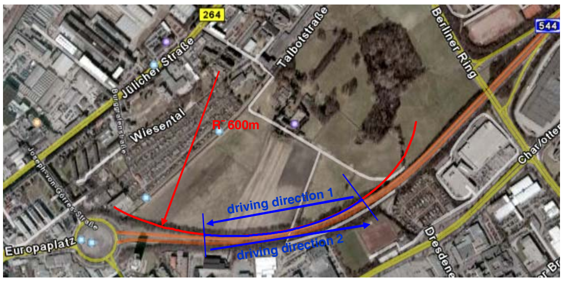


**Figure 17. Curved highway segment.**

The measurement duration is 20 s and the distance between the vehicles is 15 m. The measurement data show positive values for the curvature in a range of 0.00167 $m^{-1}$. Hence the model output can be considered as correct.

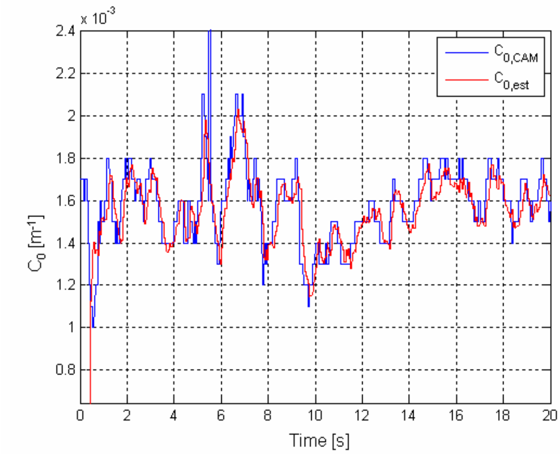


**Figure 18. Measurement results for curvature $C_{0,CAM}$ and $C_{0,est}$.**

Between 5 and 6 s the camera delivers wrong measurement values for the curvature. The street model compensates this and delivers correct values because the wrong measurement values are detected by a gating function (not described in this paper) and are not feed into the street model.

With the help of the curvature signal from the target vehicle and the implemented street model, a statement about the change of curvature is possible. The upper diagram in Figure 19 shows the curvature signal in the target vehicle, the lower shows the model based curvature change. Here no reference value was available but an estimation can be done with Equation (23). Using the curvature in the target vehicle e.g. at 18 s ($1.4 \cdot 10^{-3}$ $m^{-1}$) and the curvature in the ego-vehicle at 18 s ($1.6 \cdot 10^{-3}$ $m^{-1}$) as well as the model based curvature change ($1.3 \cdot 10^{-5}$ $m^{-2}$) in Equation (23), the resulting distance is 15.4 m, which is close to the distance between the trucks in the test (15 m). Hence the values for the curvature change can be considered as reliable.

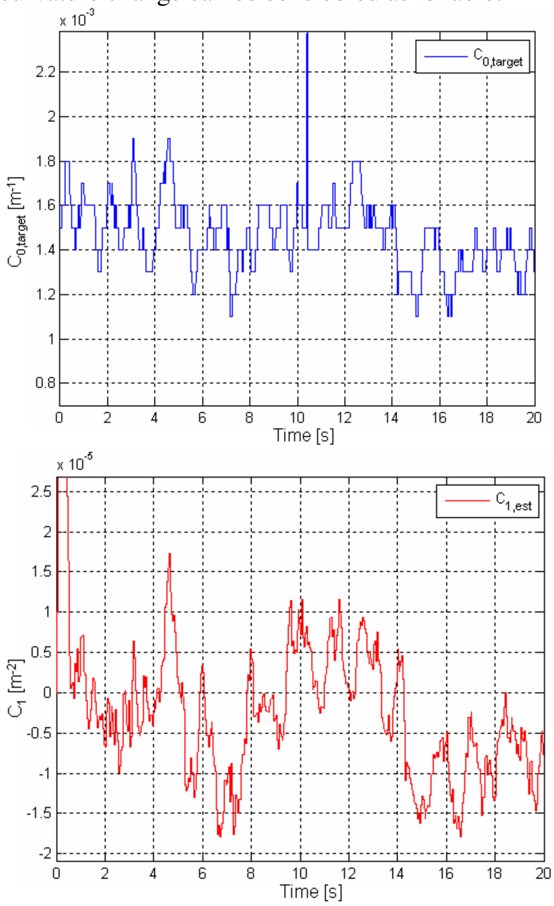


**Figure 19. Curvature signal of target vehicle (above) and estimated change of curvature (below).**

As stated above, the knowledge about the position of the target vehicle in the IDIS lidar sensor coordinate system can be used to determine a curvature $C^*_0$. Figure 20 shows the results of this approach with the curvature calculated from the target vehicle position (blue) and the curvature from the street model (red) for a test drive into direction 1 (negative curvature) with 80 kph and 30 m distance between the vehicles.

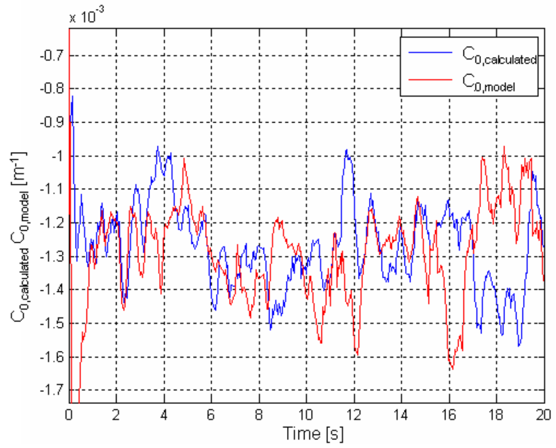


**Figure 20. Results of the corrected curveature estimation.**

After the Kalman-Filter is engaged both curvatures show comparable values, delivering a redundant signal for the curvature which can be used later in the CM system development.

## Driving tests for the determination of the quality of GPS based distance measurement

Having checked the funciotnality of the models, in a next step the accuracy of the GPS and communication based positioning is investigated. Therefore the test drives on highways are examined as a first step. With the help of offline simulations performed with the highway test data, the threshold values of the object detection algorithm are tuned.

In order to give a statement about the quality of this approach for the detection of standing objects, test drives on ika's test track with a static target vehicle are executed in a second step. The results of both experiments are presented in the following.

**Highway tests** – The following diagrams show the relative position of the target vehicle with respect to the ego-vehicle as a function of time (red graphs are the measured data of the IDIS sensor and blue graphs show the communication based position data).

The test drive depicted in Figure 21 shows an approaching maneuvre of the ego-vehicle towards the target vehicle with a starting distance of about 97 m and a relative velocity of about 7 kph. Examining both diagrams, the influence of GPS data updates can be seen (the graphs show a step). Furthermore, in the upper diagram a signal dropout at the time of 11 s (blue graph) is remarkable. This is due to a short break down of the C2C, so that the GK coordinates of the target vehicle are not updated. The lower diagram shows that a break down of the C2C

communication affects the lateral positioning not as much as the longitudinal position due to the higher velocity in longitudinal direction.
In order to acquire robust data even if C2C breaks down, a further Kalman-Filter based vehicle model of the target vehicle could be implemented in the ego-vehicle. Thus, in case of communication break down, the position of the target vehicle could be estimated model based.

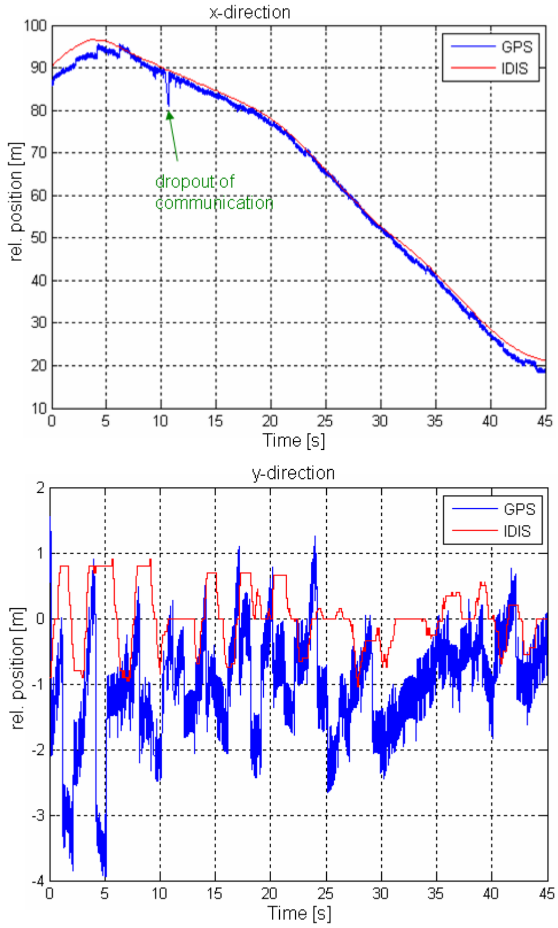


**Figure 21. Relative localisation GPS- and IDIS based.**

If the dropout from communication break down is neglected, the maximum difference between IDIS- and communication data is -2.5 m (mean value: -1.5 m) in longitudinal direction. For the lateral direction the positioning accuracy is less. At the time of 5 s the difference is -4.8 m.
Figure 22 shows two diagrams for the relative position of the target vehicle, too. Within this test a constant distance of 55 m between ego- and target vehicle was held. The positioning accuracy in lateral direction (lower diagram) did not change in comparison to the measurement described above. In contrast, in longitudinal direction a larger difference is shown. The maximum difference between the IDIS- and the communication based signal is +6.9 m (mean value: +4.85 m).
The result of the executed test drives is that the quality of the GPS based positioning is depending on various and hard to determine factors. For example, 40 % of the test drives were executed having a clear sky while 60 % of the test drives were executed when it was clouded. Within the experiments with a clear sky (e.g. the test drive in Figure 21) the measurement results are better than the experiments when it was cloudy (e.g. test drive in Figure 22) what can be caused by a better satellite reception. A further factor to the quality of the positioning accuracy is the current satellite constellation (“bad geometry”) [7].
Having analysed the measurement results for the test drives, two of five thresholds for the signal differences of the redundant signals are determined (distance in longitudinal/lateral direction).
In order to determine the remaining three thresholds (difference of velocity-, acceleration- and vehicle width signal) further simulations are carried out. Therefore the recorded sensor signals are fed in the object detection algorithm and the thresholds are varied. The effects of the threshold variation is evaluated by the help of a tool that shows the recorded scene with a birds eye view (see Figure 23).

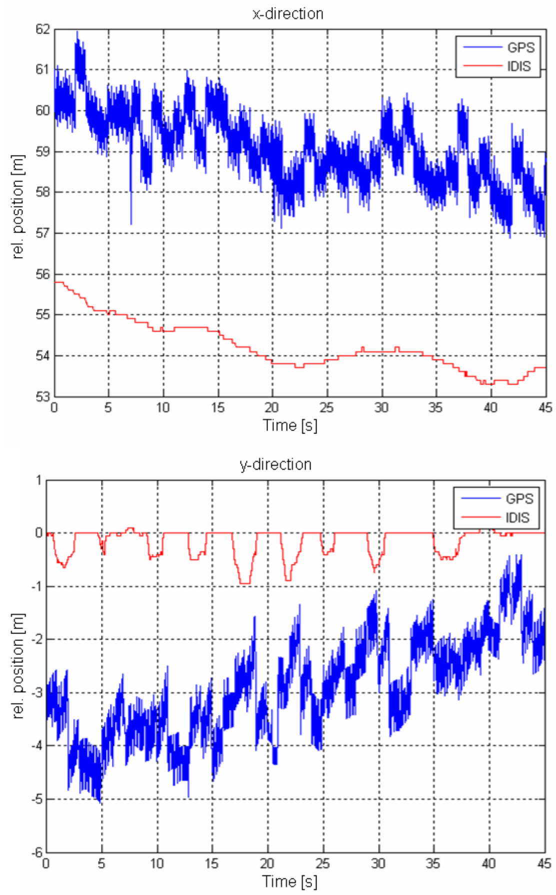


**Figure 22. Relative localisation GPS- and IDIS based.**

Displayed signals are the estimated lane trajectory of the street model as well as the lane trajectory corrected with communication data from target vehicle (red and blue graph in Figure 23). The direction of the vehicle in lane is indicated by the yellow line starting from the origin of the coordinate system. Furthermore, the IDIS data (in Figure 23 depicted as different symbols in the colours red and cyan) and the GPS and communication based position of the target vehicle (magenta coloured square) are displayed.

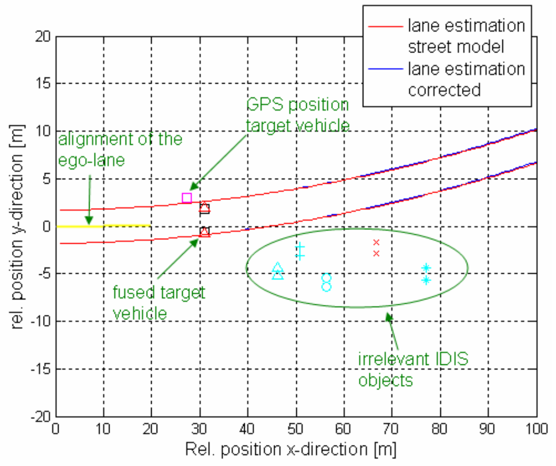


**Figure 23. Tool for test drive evaluation.**

If a relevant target is detected by the algorithm, it is marked as a black square in the bird's eye tool.
The simulations are run with different threshold constellations and the effects are observed in the evaluation tool. With this process the thresholds are determined.
One situation shown in Figure 24 could be critical for the determination of the target vehicle.

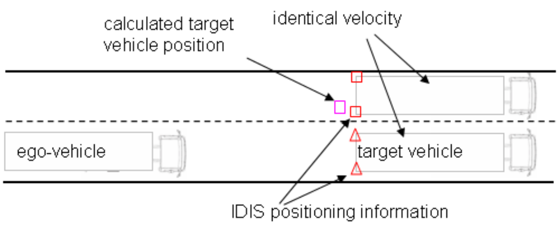


**Figure 24. Critical situation for data fusion.**

In this situation two vehicles with the identical width and velocity drive next to each other with the same distance towards the ego vehicle. The calculated position of the target vehicle differs from the position measured by the IDIS sensor. While the width, velocity, acceleration and the longitudinal distance of the two preceding vehicles is identical, the lateral position of the calculated point is different. The lateral position is located closer to the vehicle driving in the left lane. If both vehicles are equipped with a communication system, they will transmit their lane numbers to the ego-vehicle. Thus, the vehicle driving in the left lane can be regarded as not relevant by the object detection and the correct vehicle will be found.

**<u>Tests with target vehicle standing still</u>** – These experiments are executed on the test track of ika and can indentify possible factors that influence the quality of the communication based detection and ranging. Therefore two experiments were carried out with 34 measurements on two different days under different weather conditions. The procedure is shown in Figure 25.

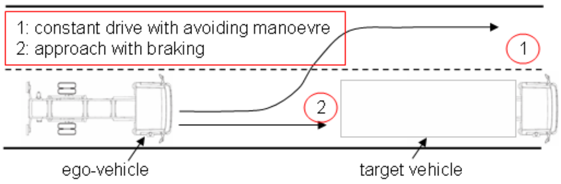


**Figure 25. Experiment procedure.**

Within experiment 1 the ego-vehicle approaches with velocities of 20, 40, 50, 60, 70 and 75 kph to the rear of the target vehicle. The ego-vehicle avoids the collision at a very late moment by steering. In the second experiment the ego-vehicle approaches with velocities of 20, 40, 50, 60 and 70 kph to the rear of the target vehicle, braking heavily at a late moment and comming to standstill behind the target vehicle.
The upper diagram in Figure 26 shows the evaluation of a test drive of the first experiment with a velocity of 50 kph. In this diagram the IDIS distance signal (red) and the calculated communication based distance (blue) are plotted as a function of the time. It is obvious that the IDIS sensor does not detect the target vehicle anymore starting from a distance of 20 m because the target passes out of the sensor detection range due to the emergency steering manoevre. In contrast, the GPS delivers distance information continuously. The difference between IDIS- and GPS based distance signal is almost constantly (7.5 m). If all test drives of experiment 1 are considered it is noticeable that the difference in the distance signal changes with the relative velocity.
In order to point out the influence of the relative velocity, the mean distance failure of different test drives for the two different test days is depicted in the lower diagram of Figure 26 as a function of the relative velocity.

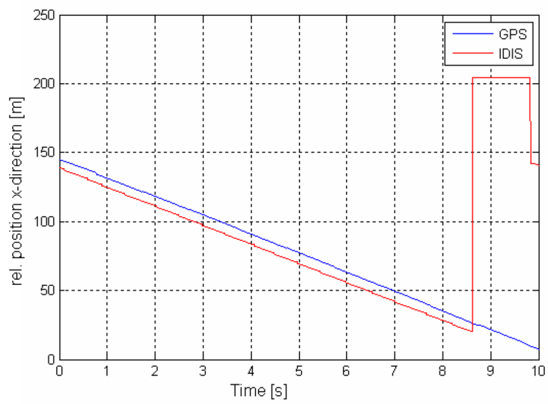

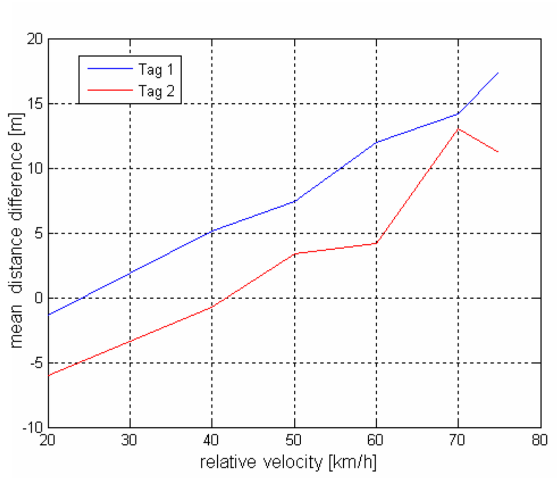


**Figure 26. Measurement evaluation of experiment 1 (above) and mean distance failure as a function of the relative velocity (below).**

Due to the seperated graphs of the tests it is obvious that the mean distance error of the first day is always larger than the error of day two. This error might be a result from different satellite constellations and different weather conditions. Furthermore, the distance error rises with increasing relative velocity.
Accordingly, the data of experiment 2 confirm the dependence of the quality of the communication based detection and ranging. Figure 27 shows the evaluation of the second test procedure with a starting ego-vehicle velocity of 70 kph. The process of the velocity signal is given by the green line in Figure 27. If the velocity decreases, the distance failure decreases, too. This proves the relative velocity dependency.

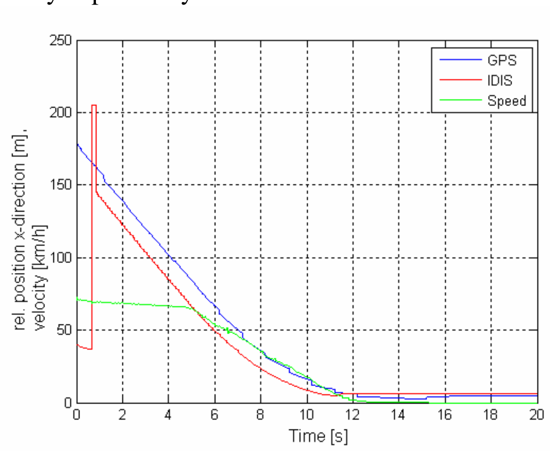


**Figure 27. Measurement evaluation of experiment 2.**

The applicability of this approach for the validation of objects standing still is hence depending of the occuring relative velocities. In the executed experiments, the developed algorithm delivered promising results up to a relative velocity of 50 kph (day one) resp. 60 kph (day two). Above this relative velocities the developed algorithm was not able to deliver dependable results due to the high difference of calculated and IDIS positioning data.

## CONCLUSION

The described system delivers robust input data for the development of collision warning (CW) and collision mitigation (CM) systems.
Therefore a GPS-Tracking was implemented, delivering a higher update rate for the vehicle position in GK coordinates. With the use of C2C, the GK coordinates and further vehicle relevant data from the preceding vehicle are transferred to the following vehicle. The run of the road trajectory is determined by ego-vehicle data and data from preceding vehicle also transmitted via C2C.
The GK coordinates from the preceding vehicle are used to determine its relative position to the ego vehicle. These data are used together with further vehicle data for the determination of the relevant target out of the data from an IDIS Lidar sensor in order to get a robust detection of stationary targets.
Within driving tests and simulations (data gained from these driving tests), the function of the detection system was tuned. It can be stated that the used concept with environmental sensors, GPS and C2C is generally suitable for the detection of stationary targets. On the other hand some limitations from the used setup and hardware must be mentioned. These limitations refer to the relative velocity between the stationary target and ego-vehicle. Within the tests a dependency of the relative velocity to the communication based position determination was found. Furthermore, the accuracy of GPS data is depending on the weather, number of satellites and satellite constellation. For future developments a DGPS system with higher accuracy should be used and a synchronisation of the C2C communication should be implemented.
Further improvements could be achieved by implementation of a bicycle model into the GPS-tracking function and the determination of a reference velocity, weighting the signals from front and rear axle speed sensors during acceleration or braking.
Despite the mentioned limitations, the presented concept was used within a CW- and CM system on the test track with promission results in [8] and we will continue the work on this topic in order to contribute to an accident reduction one day.

## REFERENCES

[1] Ellinghaus, D.; Steinbrecher, J. 2002. “Lkw im Straßenverkehr“. Eine Untersuchung über die Beziehung zwischen Lkw und Pkw-Fahrern. Uniroyal Verkehrsuntersuchung im Auftrag der Continental AG. Hannover

[2] Langwieder, K.; Knoll, P. 2006. „Der Sicherheitsaspekt in Realunfällen – Überlegungen z. volkswirtschaftlichen Nutzen von prädiktiven Fahrerassistenzsystemen“. EUROFORUM Congress

[3] Genzel, M.; Padron, J. 2005. “Adaptive Cruise Control“. Autonome Fahrzeuge Seminar. Freie Universität Berlin

[4] Southall, B.; Taylor, C. 2000. “Stochastic road shape estimation”. GRASP Laboratory, University of Pennsylvania, Philadelphia, PA 19104. www.cis.udel.edu/~cer/arv/readings/paper_southall.pdf, called: 26.03.08. Philadelphia, USA

[5] RAS-L-1 1995. “Richtlinien für die Anlage von Straßen RAS Teil: Linienführung RAS-L”. Forschungsgesellschaft für Straßen- und Verkehrswesen. Cologne, Germany

[6] Föllinger, O. 1990. “Regelungstechnik: Einführung in die Methoden und ihre Anwendung”. Hüthig, Heidelberg 1990

[7] Bozkurt, F. 2008. “Development and integration of a digital card module into a sensor fusion system”. Mini Thesis, ika - Institut für Kraftfahrzeuge Aachen, RWTH Aachen University, Aachen, Germany

[8] Wimmershoff, M. 2008. “Aufbau eines kommunikations- und umfeldsensorbasierten Collision Mitigation Systems für Nutzfahrzeuge”. Master Thesis, ika - Institut für Kraftfahrzeuge Aachen, RWTH Aachen University”, Aachen, Germany

# Universal Medical Rescue Protocol Changed: "High Speed Auto Crash" Changed to "High Risk Auto Crash" in the Field Triage Decision Scheme.

**Stewart C. Wang, MD, PhD**
Program for Injury Research and Education (UMPIRE)/University of Michigan Medical School
United States
**Scott M. Sasser, MD**
Emergency Medicine/Emory University School of Medicine
United States
**Gregory J. Jurkovich, MD**
Harborview Medical Center/University of Washington
United States

Paper Number 09-0207

## ABSTRACT

At a crash scene, EMS providers must not only determine the severity of injury and initiate medical management, but also identify the most appropriate transport destination facility through a process called "field triage." Proper decision making has a very significant impact on the outcome of injured subjects. Step III of the Field Triage Decision Scheme addresses mechanisms of injury and previously included "High Speed Auto Crash" as supported by initial estimated speed >40 MPH, major auto deformity >20 inches and intrusion into passenger compartment > 12 inches.

To take into account recent changes in trauma systems development and vehicle safety engineering and telemetry capabilities, the universally used Field Triage Decision Scheme was revised by a National Expert Panel organized by the Centers for Disease Control and Prevention. An extensive review of published evidence as well as analysis of crash injury databases was performed. New criteria targeted a 20% positive predictive value for Injury Severity Score greater than 15 (ISS>15) since more severely injured patients benefit most from transport to the highest level of trauma care. "High Speed Auto Crash" was revised to "High Risk Auto Crash" as supported by intrusion >12 inches at the occupant site or >18 inches anywhere in the vehicle as well as field telemetry consistent with high risk of injury. Rollover events and prolonged extrication were removed as criteria while death in the same occupant compartment was retained. The occupant ejection criterion was changed to specify both partial and complete ejection.

The recent revision of the universally used Field Triage Decision Scheme has potential to greatly improve rescue and treatment of crash injury victims. The addition of "vehicle telemetry consistent with high risk of injury" provides a tremendous opportunity for the automotive and medical communities to work co-operatively to improve crash safety.

## INTRODUCTION

Crash injuries are a major global public health problem. Each year, nearly 1.2 million people worldwide are killed in road traffic crashes and 20 million to 50 million more are injured. Crash injuries account for 2.1% of global mortality and 2.6% of all disability-adjusted life years (DALYs) lost. Without appropriate action, by 2020, road traffic injuries are predicted to be the third leading contributor to the global burden of disease. The economic cost of road traffic crashes is enormous. Globally it is estimated that US$518 billion is spent on road traffic crashes (1).

When someone is injured in a motor vehicle collision (MVC), the responding emergency medical services (EMS) providers must provide emergency care at the scene and then transport the patient to a health-care facility for further evaluation and treatment. "Field triage" is the process by which EMS responders determine the facility to which an injured patient should be transported. Although all emergency departments provide basic emergency services, certain hospitals, known as "trauma centers", have additional expertise and equipment for treating severely injured patients. In the United States, trauma centers are classified by the American College of Surgeons Committee on Trauma (ACS-COT) depending on the scope of resources and services available, ranging from Level I, which provides the highest level of care, to Level IV.

Whether an injured patient is triaged for transport to an appropriate level of care facility or not can have a very significant impact on that patient's subsequent morbidity and mortality. Experience with field triage has confirmed the importance of destination decisions in trauma care. The National Study on the Costs and Outcomes of Trauma (NSCOT) recently evaluated the effect of trauma center care on mortality in moderately to severely injured patients; the study found a 25% reduction in mortality for severely injured patients who received care at a Level I trauma center rather than at a non-trauma center (2). This study examined data from Level I trauma centers and large non-trauma center hospitals (i.e., hospitals that treated ≥25 major trauma patients each year) in 15 metropolitan statistical areas in 14 states. Complete data for 1,104 patients who died in the ED or hospital were compared with 4,087 selected patients who were discharged alive. After adjusting for differences in case mix, including age, comorbidities, and injury severity, the researchers found that 1-year mortality was lower among severely injured patients treated at Level I trauma centers (10.4%) than those treated at large non-trauma center hospitals (13.8%) (relative risk [RR] = 0.75; 95% CI: 0.6–1.0). Those treated at Level I trauma centers also had lower in-hospital mortality (RR = 0.8; 95% CI: 0.8–1.0), fewer deaths at 30 days after injury (RR = 0.8; 95% CI: 0.6–1.0), and fewer deaths at 90 days after injury (RR = 0.8; 95% CI: 0.6–1.0).

While it may seem easiest to transport all injured patients to trauma centers, trauma centers are a limited resource that can be overwhelmed. Furthermore, the treatment delays that result when injured patients are transported greater distances to trauma centers when sufficiently capable non-trauma centers are in closer proximity may worsen the clinical outcome of a subset of patients. Greater transport distances also place a very significant work burden on EMS responders, particularly in rural areas. Patients with less severe injuries might therefore be served better by transport to a closer ED. Transporting all injured patients to Level I trauma centers, when many do not require that high a level of resources and expertise, unnecessarily burdens those facilities and makes them less available for the most severely injured patients.

The initial recommendations from the ACS-COT in *Field Categorization of Trauma Patients* in 1976 (3) did not specify triage criteria, but they did contain physiologic and anatomic measures that allowed stratification of patients by injury severity. At that time, the ACS-COT developed guidelines for the verification of trauma centers, including standards for personnel, facility, and processes deemed necessary for the optimal care of injured persons. Subsequent studies in the 1970s and early to middle 1980s showed a reduction in mortality in those regions with specialized trauma centers (4-6). These studies led to a national consensus conference in 1987 that resulted in the first ACS field triage protocols, known as the "Triage Decision Scheme" for trauma patients. Since 1987, this Decision Scheme has served as the basis for the field triage for trauma patients in the majority of EMS systems in the United States. Individual EMS systems may adapt the Decision Scheme to meet the demands of the operational context in which they function. For example, the Decision Scheme may be modified to a specific environment (densely urban or extremely rural), to resources available (presence or absence of a specialized pediatric trauma center), or at the discretion of the local medical director. This Decision Scheme has been widely adopted by EMS systems around the world.

The "accuracy" of field triage is the degree of match between severity of injury and level of care. Maximally sensitive triage would mean that all patients with injuries appropriate to a Level I or Level II trauma center would be sent to such centers. Maximally specific triage would mean that no patients who could be treated at a Level III or Level IV center or community ED would be transported to a Level I or Level II center. Triage that succeeded in transporting only patients with high injury severity to a Level I or Level II center would maximize the positive predictive value (PPV) of the process, and triage that succeeded in transporting only low injury severity patients to a Level III, IV, or community ED would maximize the negative predictive value (NPV).

Ideally, all persons with severe, life-threatening injuries would be transported to a Level I or Level II trauma center, and all persons with less serious injuries would be transported to lower-level trauma centers or community EDs. Unfortunately, patient differences, occult injuries, and the complexities of patient assessment in the field make it impossible to attain perfect accuracy in triage decisions. Inaccurate triage that results in a patient who requires higher-level care not being transported to a Level I or Level II trauma center is termed "undertriage." The result of undertriage is that a patient does not receive the specialized trauma care required. "Overtriage" occurs when a patient who does not require care in a higher-level trauma center is nevertheless transported to such a center, thereby unnecessarily consuming scarce resources. In the triage research literature, all of these measures—sensitivity, specificity, PPV, NPV, undertriage, and overtriage—along with measures of association such as the odds ratio, are used to assess the effectiveness of field triage.

Like sensitivity and specificity applied to screening tests, reductions in undertriage are usually accompanied by increases in overtriage, and vice versa. Because the potential harm associated with undertriage (i.e., causing a patient in need of trauma center care not to receive appropriate care) is high and could result in death or substantial morbidity and disability, trauma systems frequently err on the side of minimizing undertriage rather than minimizing overtriage. Target levels for undertriage rates within a trauma system might range from 1% to 5% of patients requiring Level I or II trauma center care, depending on the criteria used to determine the undertriage rate (e.g., death, ISS) (7). Acceptable overtriage rates vary, but might range from 25% to 50% (7). As field triage continues to change on the basis of new research findings, overtriage rates might be reduced while maintaining low undertriage rates so that limited health care resources can be optimally used.

## METHODS

The National Expert Panel of Field Triage is comprised of three dozen individuals with expertise in acute injury care representing a broad range of interested parties, including EMS providers and medical directors, emergency medicine physicians and nurses, adult and pediatric trauma surgeons, the automotive industry, public health, and Federal agencies. This Panel is responsible for periodically reevaluating the Decision Scheme, determining if the criteria are consistent with current scientific evidence and compatible with advances in technology (e.g., vehicular telemetry), and, as appropriate, recommending revisions to the Decision Scheme. In May 2005, with support from NHTSA's Office of Emergency Medical Services, the Centers for Disease Control and Prevention (CDC) convened the Panel to evaluate and revise the 1999 Decision Scheme. The Panel recognized that peer-reviewed studies would be the preferred basis for its decisions regarding revision of the Decision Scheme, but noted that literature that specifically addresses or supports the Decision Scheme or its component criteria is sparse. Thus, the Panel decided to use multiple approaches to identify as much relevant published literature as possible and to consider other sources of evidence (e.g., consensus statements, policy statements). Finally, when definitive research, consensus, or policy statements were lacking, the Panel based revisions and recommendations on the expert opinion of its members.

In preparation for the first meeting of the Panel, a structured literature review (8) was performed which examined the entire Decision Scheme and each of its component steps. MEDLINE was used and English-language articles published between 1966 and 2005 were searched using the Medical Subject Headings (MeSH) "emergency medical services," "wounds and injury," and "triage." Additionally, the reference sections of identified papers were searched to identify other potential articles. A total of 542 titles were identified, of which 80 relevant articles were subsequently reviewed and presented to the Panel at its first meeting. During the subsequent two-year revision process, panel members also identified additional relevant literature that had not been examined during the structured review. Primary emphasis was placed on articles published since the development of the 1999 version of the Decision Scheme.

At its initial meeting, the Panel determined that the limited evidence was most compelling in support of the physiologic (Step One) and anatomic (Step Two) criteria of the Decision Scheme. Agreement was unanimous that the mechanism of injury criteria (Step Three) needed revision, and approximately half of the

Panel recommended that the special considerations step (Step Four), which addresses comorbidity and extremes of age, be revised. Ultimately, the Panel elected to undertake limited revisions of the physiologic and anatomic steps and more substantive revision of the mechanism of injury and special considerations steps. Working subgroups of the Panel then conducted further detailed review of the literature and developed recommendations regarding individual components of the Decision Scheme, focusing on the determination of the accuracy of existing criteria and on identifying new criteria needed for both Steps Three and Four of the Decision Scheme.

The working subgroups used ISS >15 generally as the threshold for identifying severe injury; however, other factors (e.g., need for prompt operative care, intensive care unit [ICU] admission, case fatality rates) were also considered. Varying methodologies and different analyses were used to determine the appropriateness of individual mechanism of injury (Step Three) criteria (e.g., ISS or resource utilization). Thus, a threshold of 20% PPV to predict severe injury (ISS >15), major surgery, or ICU admission was used to place new criteria into discussion for inclusion as mechanism of injury criteria. PPV <10% was used as a threshold for placing existing mechanism of injury criteria into discussion for removal from the Decision Scheme. In selecting the PPV thresholds, the Panel recognized the limitations of data available in the relevant literature. In addition to the criteria automatically placed into discussion based on PPV <10% or >20%, Panel members also could nominate criteria having PPV 10%–20% for further discussion.

The recommendations of the working subgroups were presented to the entire Panel in April 2006 for discussion, minor modification, and formal adoption as revisions to the Decision Scheme. Final consensus on the recommendations in the Decision Scheme was reached on the basis of supporting or refuting evidence, professional experience, and the judgment of the Panel. The revised Decision Scheme (Figure 1), with a draft description of the revision process, was distributed to relevant associations, organizations, and agencies representing acute-injury care providers and public health professionals for their review and endorsement. Following endorsement by multiple organizations, the Decision Scheme was published in 2006 edition of the American College of Surgeons' *Resources for the Optimal Care of the Injured Patient*.

The definitive detailed description of the process of revision and the rationale behind the new decision scheme was published in the medical literature in January 2009 (9). Readers should refer to this definitive monograph for information regarding the full extent of changes made to the Field Triage Decision Scheme. In order to increase awareness within the international automotive safety community of these important changes to the Decision Scheme, this current manuscript for the 21st Enhanced Safety of Vehicles Conference focuses only on the changes to Step Three (Mechanism of Injury) criteria relevant to injured MVC occupants.

## RESULTS

### Criterion Deleted: Extrication Time >20 Minutes

In determining whether to retain extrication time >20 minutes as a criterion in the 2006 Decision Scheme, the Panel recognized potential problems with field use of this criterion. It is difficult for EMS personnel to determine exact times while managing the scene of a crash and assessing and treating vehicle occupants. Adverse weather conditions and darkness can further complicate matters. Additionally, because most EMTs are trained only to do light extrication, and must call someone else for heavy rescue, it is unclear when EMS personnel should "start the clock" for the 20-minute time frame.

The Panel recognized that, although lengthy extrication time may be indicative of increasing injury severity, the new vehicle construction and improved occupant protection systems in modern automobiles appear to be causing an increase in the number of non-seriously injured patients who require >20 minutes for extrication. Although occupants may require extrication due to lower extremity injuries, they may not have sustained serious life-threatening injuries to the head or torso due to improved occupant protection systems. The Panel determined that the changes made to the triage protocol for cabin intrusion adequately addressed issues relevant to extrication time, and elected to delete extrication time as a criterion (Table 2, Figure 1). This also decreases the number of criteria with which EMS personnel must contend in the time-sensitive decision making required on the scene of a motor vehicle crash.

**Table 1.**

**Old Step 3 (Mechanism of Injury) Criteria**

| |
|---|
| *High speed auto crash*<br>*Initial speed > 40 mph*<br>*Major auto deformity > 20 inches*<br>*Intrusion into passenger compartment > 12 inches* |
| *Ejection from automobile* |
| *Death in same passenger compartment* |
| *Extrication time >20 minutes* |
| *Rollover* |
| Falls > 20 feet |
| Auto-pedestrian/auto-bicycle injury with significant (>5 mph) impact |
| Pedestrian thrown or run over |
| Motorcycle crash > 20 mph or with separation of rider from bike |

**Table 2.**

**Current Step 3 (Mechanism of Injury) Criteria**

| |
|---|
| *High-Risk Auto Crash*<br>*Intrusion: >12 in. occupant site or >18 in. any site*<br>*Ejection (partial or complete) from automobile*<br>*Death in same passenger compartment*<br>*Vehicle telemetry data consistent with high risk of Injury* |
| Falls<br>Adults: >20 ft. (one story = 10 ft.)<br>Children: >10 ft. or 2–3 times child's height |
| Auto versus pedestrian/bicyclist thrown, run over, or with significant impact (>20 mph) |
| Motorcycle crash >20 mph |

**Criterion Deleted: Rollover Crash**

Published data indicate that rollover crash event has a PPV for severe injury of <10%. A multivariate analysis of 621 crashes indicated that rollover crash was not associated with ISS >15 (10). Analysis of contemporary NASS CDS research confirmed that rollover crash (in the absence of ejection) was not associated with increasing injury severity (AIS >3) although rollovers with occupant ejection were clearly associated with increasing injury severity (11). Review of current NASS CDS data also showed that a >20% risk of ISS >15 was not associated with the number of quarter turns in a rollover crash, nor the landing position of the vehicle or maximum vertical or roof intrusion. (11)

The increased injury severity associated with rollover crashes is seen when an occupant is partially or completely ejected from the vehicle, which most frequently occurs when restraints are not used. The decision was made to broaden the ejection criterion to include both partial and complete ejection for transport to a trauma center as a mechanism of injury associated with high-risk auto crash (see below). As a result of these findings, the Panel concluded that rollover crash, in and of itself, is not associated with increasing injury severity and should not stand as a separate criterion. The Panel chose to delete rollover crash criterion from the 2006 Decision Scheme (Table 2, Figure 1).

**Criterion Retained: Ejection (Partial or Complete) from Automobile**

There was evidence to support that ejection is associated with increased severity of injury. A multivariate analysis of data collected from 1996–2000 at the Royal Melbourne Hospital in Victoria, Australia, examined 621 crashes and found that ejection from the vehicle was associated with major injury defined as ISS >15, ICU admission >24 hours requiring mechanical ventilation, urgent surgery, or death (OR = 2.5; CI: 1.1–6.0) compared with crashes without ejection (10). A retrospective evaluation of NASS data collected during 1993–2001 was conducted to determine the crash characteristics associated with significant chest and abdominal injuries; this evaluation indicated that the predictive model that produced the best balance between sensitivity and specificity included ejection as a variable (12). A person who has been ejected from a vehicle as a result of a crash has been exposed to a significant transfer of energy with the potential to result in severe life- or limb-threatening injuries. Lacking the protective effects of vehicle restraint systems, occupants who have been ejected may have struck the interior many times prior to ejection (13). Further, ejection of the patient from the vehicle increases the chance of death by 25 times, and one of three ejected victims sustains a cervical spine fracture (13). No literature reviewed argued conclusively for removal of this criterion. Therefore, on the basis of the available, albeit limited, evidence, combined with the Panel's experience, ejection from the vehicle was retained as a criterion (Table 2, Figure 1).

The Panel further concluded that, because the literature reviewed showed that partial or complete ejection is associated with severe injury, ICU admission, urgent surgery, and death, even if these patients do not meet physiologic or anatomic criteria, they still warrant a trauma center evaluation based upon mechanism only. Additionally, ejections of vehicle occupants are not that frequent. Transporting all such patients for evaluation would not be expected to overburden the system. These patients may be transported to the closest appropriate trauma center, which, depending on the trauma system, need not be the highest level trauma center.

**Criterion Retained: Death in Same Passenger Compartment**

In the context of a MVC, death of an occupant in a vehicle is highly indicative that a significant force has been applied to that vehicle and all of its occupants. A prospective study of MVC victims in Suffolk County, New York, indicated that death of an occupant in the same vehicle was associated with increased odds for major surgery or death (AOR = 39.0; CI: 2.7–569.6) and ISS >15 (AOR = 19.8; CI: 1.1–366.3) (14). A prospective study of 1,473 patients, which did not account for the impact of physiologic or anatomic criteria, indicated that 3 of 14 occupants in a vehicle with a fatality had ISS >15, resulting in PPV of 21.4% for severe injury by this mechanism (15)). A review of data concerning 621 crash victims indicated that occupants of vehicles in which a fatality occurred comprised 11% of the patients evaluated and 7% of the patients with major injury, but fatality of an occupant was not statistically associated with major injury (10). In its discussions, the Panel noted that two of the three studies cited above demonstrated a PPV >20% for ISS >15, as well as increased odds for major surgery or death of occupants in a vehicle in which a fatality occurs. Although the remaining study did not show a statistical association with major injury, this single study was not compelling enough to delete this criterion. Panel members affirmed that, in their clinical experience, death of an occupant in a vehicle is associated with a risk of severe injury to any surviving occupant.

After reviewing the evidence, the Panel concluded that death in the same passenger compartment should be retained as a criterion for the 2006 version of the Decision Scheme (Table 2, Figure 1). Surviving passengers should be transported to the closest appropriate trauma center. As the number of patients who fall into this category is small, such requirement for transport would not overburden the system.

**Criterion Modified: Intrusion >12 inches at Occupant Site, or >18 inches at Any Site**

Evidence examined in consideration of this criterion included the 2003 retrospective study of 621 MVC victims which did not account for physiologic or anatomic criteria reported that cabin intrusion >30 cm (>11.8 inches) was associated in univariate analysis ($p$ = <0.0001) with major injury, defined as one of the following: ISS >15; ICU admission for >24 hours requiring mechanical ventilation; urgent cranial, thoracic, abdominal, pelvic-fixation, or spinal-fixation surgery; or death. However, this association was not statistically significant in multivariate analysis (OR 1.5; 95% CI: 1.0–2.3; $p$ = 0.047) (*90*). Similarly, a univariate analysis of New York State data that examined the incremental benefit of the individual ACS triage criteria, identified increased odds of severe injury (ISS >15) for 30 inches of vehicle deformity (OR = 4.0; 95% CI: 2.1–7.8), 24 inches of intrusion on the side of the vehicle opposite the victim (OR = 5.2; 95% CI: 2.6–10.4), and 18 inches of intrusion on the same side of the vehicle as the victim (OR = 7.1; 95% CI: 3.8–13.0) (*58*). However, none of these findings was statistically significant in multivariate analysis.

Data from the National Automotive Sampling System Crashworthiness Data System (NASS CDS), which includes statistical sampling of all crashes occurring in the United States, indicated that a very large crush depth, 30 inches in frontal collisions and 20–24 inches in side-impact collisions, was needed to attain a PPV of 20% for ISS >15 injury to occupants (16). External crush of such great extent is difficult to measure in the field without reference information from an undamaged exemplar vehicle. The Panel also recognized that recent changes in vehicle design and construction have likely reduced the effect of crush on the risk for severe injury in crashes. Whereas older vehicles were more likely to transmit the kinetic energy of crashes to vehicle occupants and cause severe injuries, newer vehicles are designed to crush externally and absorb energy, protecting passenger compartment integrity and occupants. Additionally, the Panel took note of the difficulty of using deformity or crush criteria in the field. Crash sites are difficult environments in which to estimate such measures, and little might be left of a vehicle to serve as a reference point for determining crush depth. For example, in one study, only 1.0% of 94 cases with 30 inches or more of deformity were documented by EMS personnel (17). The Panel concluded from these three studies that external vehicle crush depth or deformity was not a useful indicator for severe injury.

The Panel reviewed NASS CDS data from 1997-2005 which showed that intrusion of 12 inches at the occupant site or 18 inches of intrusion at any site had a PPV of 20% for ISS>15 for MVC occupants (16). Similarly, stuck side lateral intrusion of 12 inches was needed to attain a PPV of 20% for ISS>15 to lateral impact crash occupants (16). Furthermore, extensive anecdotal experience in trauma practice indicates that increasing cabin intrusion is indicative of an increasing amount of force upon the vehicle and potentially upon the occupant. Also, side-impact intrusions could present special clinical concerns that had not been fully recognized in existing research, given the limited space between the impact and occupant. Finally, although modern vehicles have better energy-absorbing capability, vehicle incompatibility (crash involving a large vehicle versus a small vehicle) might be increasingly significant in the level of vehicle intrusion in crashes.

**Criterion Added: Vehicle Telemetry Data Consistent with High Risk of Injury.**

In earlier versions of the Decision Scheme, initial vehicle speed > 40 mph, vehicle deformity >20 inches, and intrusion >12 inches for unbelted occupants were included as mechanism of injury criteria. NASS data indicate that risk for injury, impact direction, and increasing crash severity are linked (16). An analysis of 621 Australian MVCs indicated that high-speed impacts (>60 km/hr [>35 mph]) were associated with major injury, defined as ISS >15, ICU admission >24 hours requiring mechanical ventilation, urgent surgery, or death (OR = 1.5; 95% CI: 1.1–2.2) (10). Previously, the usefulness of vehicle speed as a criterion had been limited because of the challenges to EMS personnel to estimate impact speed accurately. However, new Advanced Automatic Collision Notification (AACN) technology installed in some automobiles, now in approximately six million vehicles in the United States and Canada, (18) can identify vehicle location, measure change in velocity ("delta V") during a crash, and detect crash principal direction of force (PDOF), airbag deployment, rollover, and the occurrence of multiple collisions (18, 19). As a result, and in recognition that this information might become more available in the future, vehicle telemetry data consistent with a high risk for injury (e.g., change in velocity, principal direction of force) was added as a triage criterion (Table 2, Figure 1). This criterion was intentionally left nonspecific at the time of publication, as this emerging area requires additional evaluation of available data to define the exact components (e.g., belt use, delta V, PDOF) consistent with a high risk for injury. CDC is working with the automotive industry and experts in public health, public safety, and health care to examine how data collected by AACN systems can be used to predict injury severity, conveyed to EMS services and trauma centers, and integrated into the field triage process.

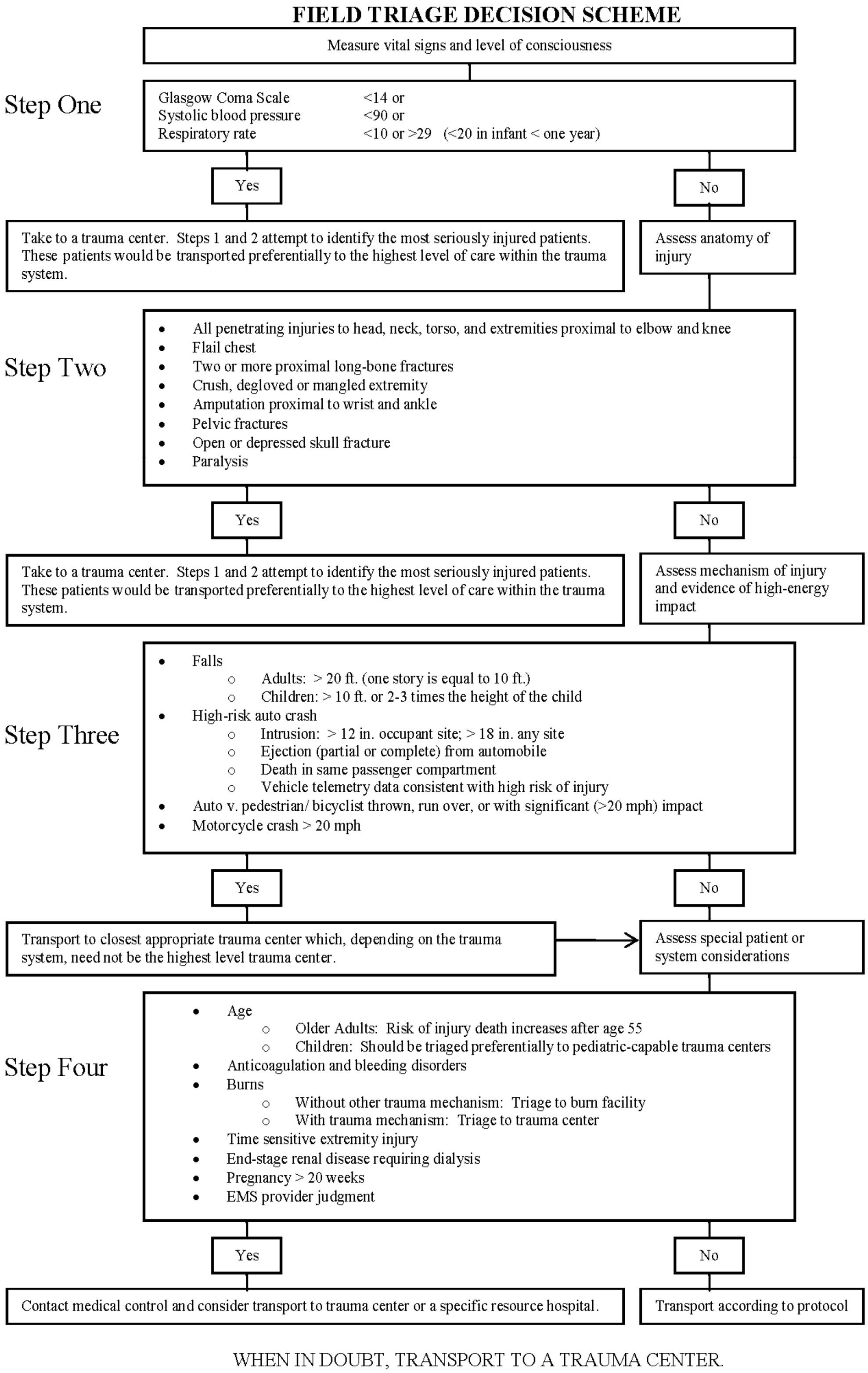


**Figure 1. New field triage decision scheme**

## CONCLUSION

The universally used Field Triage Decision Scheme was recently revised using a National Expert Panel convened by the Centers for Disease Control and Prevention, the National Highway Traffic Safety Administration and the American College of Surgeons Committee on Trauma. This Panel reviewed the available evidence and proposed revisions which were endorsed by multiple professional organizations.

Implementation and updating of these protocols at the local level will require a substantial educational and informative effort to ensure its wide scale implementation. The CDC, with additional funding from NHTSA, is developing an educational toolkit for State and local EMS medical directors, State EMS Directors, EMS providers, and public health officials. The tool kit will provide teaching aids to help EMS providers understand why the Decision Scheme was revised and how those revisions can be tailored to the needs of their communities. CDC, through its partner organizations, will distribute the tool kit to EMS jurisdictions throughout the United States. This toolkit also will be available online from CDC at http://www.cdc.gov for downloading and ordering free of charge. Providing the revised Decision Scheme to EMS administrators and providers should improve care for trauma patients nationwide and lead to reduced morbidity, mortality, disability, and costs from injuries.

The evaluation of trauma care in the prehospital environment and the evidence supporting appropriate care is necessarily an ongoing process. The current revisions to the Field Triage Decision Scheme were made on the basis of the best evidence currently available. Limitations in available data clearly indicate the need for additional research. Conducting research in the prehospital environment and in EMS presents multiple challenges, including a lack of trained investigators, legal and regulatory barriers, lack of appreciation and interest in research among EMS providers, lack of funding, and limited infrastructure and information systems to support research efforts (20, 21). Efforts are underway to address these barriers, including efforts to prioritize research, as in CDC's Acute Injury Care Research Agenda: Guiding Research for the Future (22) and The National EMS Research Strategic Plan (23), as well as in development of new databases that can provide more useful information and support data-driven changes (e.g., NTDB, National EMS Information System [NEMSIS]) (24). Additional research efforts specifically related to field triage are needed, including cost-effectiveness research. Additional funding targeting research into triage decisions and triage criteria will be necessary to support these efforts. Also, research in triage represents an important area in which public health and EMS can collaborate to improve trauma surveillance and data systems and develop the methodologies needed to carry out the continuing analysis and evaluation of the 2006 Decision Scheme and its impact on the care of the acutely injured.

For the automotive safety community, the new Decision Scheme as well as the open, thorough and inclusive process used to revise it demonstrates clear recognition that there are many stakeholders in efforts to enhance vehicle safety. The revisions and their implementation at the local level demonstrate that the EMS and trauma communities are adjusting their protocols and procedures to account for advances in vehicle engineering and occupant protection. Improved utilization of limited and expensive health care resources will help to decrease the societal costs of motor vehicle crash injuries. The insertion of an open criterion of "vehicle telemetry consistent with high risk of injury" provides the automotive community with a tremendous opportunity to explore technological innovations that can improve safety and crash outcomes. Coupled with planned research efforts by CDC, NHTSA as well as regional EMS and trauma systems to prospectively collect data regarding the effect and efficacy of the new triage criteria, the automotive community will soon have access to much better real-life crash information. This rapid feedback regarding vehicle safety performance will guide and shorten the cycle of improvements necessary for the enhanced safety of vehicles.

## ACKNOWLEDGEMENTS

The authors would like to acknowledge the contributions of Richard Hunt, Robert Lange and William Ball in the preparation of this paper.

**REFERENCES**

1. Peden, M. Global Collaboration on Road Traffic Injury Prevention. 2005. International Journal of Injury Control and Safety Promotion. June: 12:85-91.

2. MacKenzie EJ, Rivara FP, Jurkovich GJ, et al. A national evaluation of the effect of trauma center care on mortality. 2006. New England Journal of Medicine. 354:366-78.

3. Mackersie RC. History of trauma field triage development and the American College of Surgeons criteria. 2006. Prehospital Emergency Care. 10:287-94.

4. Guss DA, Meyer FT, Neuman TS, et al. The impact of a regionalized trauma system on trauma care in San Diego County. 1989. Annals of Emergency Medicine. 18:1141-5.

5. Campbell S, Watkins G, Kreis D. Preventable deaths in a self-designated trauma system. 1989. The American Surgeon. 55:478-80.

6. West JG, Trunkey DD, Lim RC. Systems of trauma care: a study of two counties. 1979. Archives of Surgery. 114:455-60.

7. American College of Surgeons. Resources for the optimal care of the injured patient: 2006. Chicago, IL: American Colleges of Surgeons; 2006.

8. Lerner EB. Studies evaluating current field triage: 1966-2005. 2006. Prehospital Emergency Care. 10:303-6.

9. Sasser SM, Hunt RC, Sullivent EE, Wald MM, Mitchko J, Jurkovich GJ, Henry MC, Salomone JP, Wang SC, Galli RL, Cooper A, Brown LH, Sattin RW. Guidelines for field triage of injured patients: Recommendations of the National Expert Panel on Field Triage. 2009 Morbidity and Mortality Weekly Report. 58(RR-1):1-35.

10. Palanca S, Taylor DM, Bailey M, Cameron PA. Mechanisms of motor vehicle accidents that predict major injury. 2003. Emergency Medicine (Fremantle). 15: 428-8.

11. Eigen AM. Rollover crash mechanisms and injury outcomes for restrained occupants. Washington, DC: National Highway Traffic Safety Administration; 2005. Available at http://www-nrd.nhtsa.dot.gov/Pubs/809894.PDF.

12. Nirula R, Talmor D, Brasel K. Predicting significant torso trauma. 2005. Journal of Trauma. 59:132-5.

13. Getz SA, Rodriguez EK. Trauma. In: Elling B, Smith M, Pollak AN, eds. Nancy Caroline's emergency care in the streets. 6th ed. Boston: Jones and Bartlett Publishers; 2008:17.5-17.29.

14. Henry MC, Hollander JE, Alicandro JM, Cassara G, O'Malley S, Thode HC. Incremental benefit of individual American College of Surgeons trauma triage criteria. 1996. Academic Emergency Medicine. 3:992-1000.

15. Knopp R, Yanagi A, Kallsen G, Geide A, Doehring L. Mechanism of injury and anatomic injury as criteria for prehospital trauma triage. 1988. Annals of Emergency Medicine. 17:895-902.

16. Wang, SW. Review of NASS CDS and CIREN data for mechanism criteria for field triage. Presented at the National Expert Panel on Field Triage meeting, Atlanta, Georgia; November 15, 2005.

17. Henry MC. Trauma triage: New York experience. 2006. Prehospital Emergency Care. 10:295-302.

18. Ball WL. Telematics. 2006. Prehospital Emergency Care. 10:320-1.

19. Hunt RC. Emerging communication technologies in emergency medical services. 2002. Prehospital Emergency Care. 6:131-6.

20. Jurkovich GJ, Mock C. Systematic review of trauma system effectiveness based on registry comparisons. 1999. Journal of Trauma. 47(Suppl 3):S46-55.

21. Sayre MR, White LJ, Brown LH, McHenry SD: The National EMS Research Agenda Executive Summary. 2002. Annals of Emergency Medicine. 40:636-43.

22. CDC. CDC acute injury care research agenda: guiding research for the future. Atlanta, GA: US

Department of Health and Human Services, CDC; 2005. Available at http://www.cdc.gov/ncipc/dir/ARagenda.htm.

23. Sayre MR, White LJ, Brown LH, McHenry SD, for the National EMS Research Strategic Plan Writing Team. The National EMS Research Strategic Plan. 2005. Prehospital Emergency Care. 9:255-66.

24. Sattin RW, Corso PS. The epidemiology and costs of injury. In: Doll L, Bonzo S, Mercy J, Sleet D, eds. Handbook on injury and violence prevention interventions. New York, NY: Kluwer Academic/Plenum Publishers; 2006:3-19.

**FIELD TEST OF A COOPERATIVE INTERSECTION COLLISION AVOIDANCE SYSTEM FOR VIOLATIONS (CICAS-V)**

**Vicki L. Neale**
**Zachary R. Doerzaph**
Virginia Tech Transportation Institute
USA
Paper Number 09-0478

## ABSTRACT

The design objective of the Cooperative Intersection Collision Avoidance System for Violation (CICAS-V) project is to create a system that presents a timely and salient in-vehicle warning to those drivers who are predicted, by means of an algorithm, to violate a stop-sign or signal-controlled intersection. An on-road test was conducted to evaluate the CICAS-V using naïve participants to demonstrate that all systems are mature for a Field Operational Test (FOT). Data were evaluated from 72 naïve drivers representing both genders and three age groups who were placed into CICAS-V equipped vehicles to navigate a 2-hour prescribed route through equipped intersections in Virginia. During the prescribed route, drivers crossed 10 stop-controlled and 3 signal-controlled intersections equipped with CICAS-V making a variety of turn maneuvers through each for a total of 52 intersection crossings. The rate at which drivers received correct, false, and missed warnings was evaluated. Results indicate that the algorithms for both stop-controlled and signalized intersections were effective and that the prototype CICAS-V is mature for large-scale tests with naïve drivers. Participants in the study who received warnings rated the CICAS-V very favorably and felt that the system would be beneficial. Recommendations were made for continuing with an FOT. Furthermore, the methods for conducting the study were determined to be suitable for an FOT. This study marked the first field test of the CICAS-V with naïve drivers. Project participants included offices of the United States Department of Transportation, Daimler, Ford, General Motors, Honda, Toyota, and the Virginia Tech Transportation Institute.

## INTRODUCTION

Intersection crashes account for thousands of injuries and fatalities in the United States every year (National Highway Traffic Safety Administration, 2006). Drivers running stop-controlled and red-phased signalized intersections cost over $7.9 billion in economic loss each year (Najm et al., 2007). The objective of a Cooperative Intersection Collision Avoidance System for Violations (CICAS-V) is to assist drivers in avoiding intersection crashes. The basic design objective of the CICAS-V is to create a system that presents a timely and salient in-vehicle warning to those drivers who are predicted, by means of an algorithm, to violate a stop light or a stop sign. The warning is intended to elicit a behavior from the driver that will motivate him or her to respond appropriately to avoid a violation; by doing this, the driver will also avoid a potential intersection crash should cross traffic be present.

The CICAS-V project consisted of 14 tasks to complete design, development, and testing of the CICAS-V (Maile et al., in print-c). This paper describes the process and results of an on-road study to test the system. Naïve drivers were placed into CICAS-V equipped vehicles to navigate a 2-hour prescribed route through designated intersections. The following sections report the method for this task.

## METHOD

The experiment consisted of a Pseudo-Naturalistic Study (a pre-determined route on open roadways without an experimenter in the vehicle) investigating the CICAS-V in live traffic. The methods and equipment used are described in the subsequent sections.

### Drivers

Drivers were recruited through the newspaper, posted flyers, word of mouth, and the Virginia Tech Transportation Institute (VTTI) database of people who had expressed an interest in participating in studies. On initial contact (usually over the phone), individuals were screened to ensure their eligibility for the study. Eligibility criteria included restrictions barring participation by individuals with: 1) health conditions or medication intake that may interfere with their ability to operate a motor vehicle, or 2) more than two moving violations or any at-fault accidents within the previous three years. The criteria also included the requirement that drivers had to possess a valid driver's license.

**CICAS-V Equipment and Data Acquisition System (DAS)**

The following sections describe the hardware and software used. This includes the CICAS-V designed and developed, and the experimental equipment constructed, to directly support the study.

**CICAS-V Description** – The system engineering, system design, and prototype build of the CICAS-V were conducted by the Collision Avoidance Metrics Partnership Vehicle Safety Communications 2 Consortium (CAMP VSC2), which included the representatives of Ford, General Motors, Daimler, Honda, and Toyota (Maile et al., in print-c). The CICAS-V contains several components working together to predict a stop-sign or red-phased signal violation, and present a warning to the driver when appropriate. To provide context, an overview of the CICAS-V is included.

The CICAS-V is comprised of onboard equipment (OBE) and roadside equipment (RSE). As part of the OBE, the Wireless Safety Unit (WSU) developed by DENSO is the central processing component of the CICAS-V network. It is responsible for collecting data from the vehicle and sensors from which it computes an algorithm to predict when a violation may occur and, based on that prediction, issues a warning to the driver through the Driver-Vehicle Interface (DVI). The WSU receives data from the vehicle Controller Area Network (CAN), the global positioning system (GPS), and Dedicated Short Range Communications (DSRC) messages. These data are pre-processed and then evaluated in parallel with the warning algorithm. If the algorithm predicts a violation, the WSU activates the DVI.

The WSU controls the three DVI modalities – auditory, visual, and haptic. The DVI has three states: 1) an inactive state when the vehicle is not approaching an equipped intersection; 2) a visual-only indication when approaching an equipped intersection; and 3) a full warning mode that encompasses a "single stage" activation of the visual, auditory, and haptic alerts.

The auditory warning consisted of a female voice stating "Stop Light" or "Stop Sign", presented at 72.6 dBA out of the front speakers, measured at the location of the driver's head.

The visual warning is displayed by a dash-mounted icon (Figure 1) positioned at the vehicle centerline near the cowl of the windshield. As implemented in the vehicle, the visual icon was 11.6 mm (0.46 inches) high and 11.6 mm (0.46 inches) wide. It was illuminated as either steady, continuous blue (advisory), or flashing red (warning).

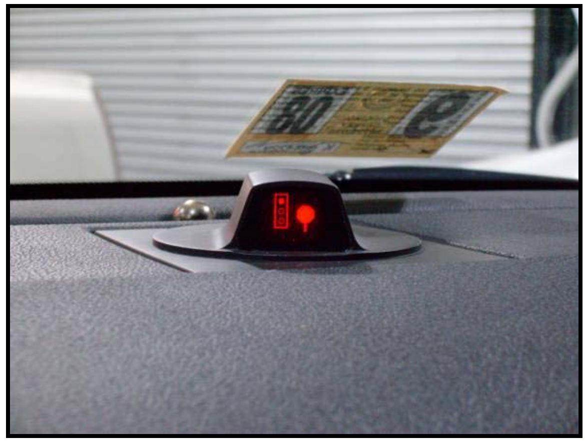

**Figure 1. The visual display is located on the dash of the experimental vehicle.**

The haptic brake pulse command was sent to the Original Equipment Manufacturer (OEM) brake controller. When the warning was activated, a single 600-millisecond (ms) brake pulse was presented in conjunction with the visual icon and an auditory warning. The brake pulse was triggered immediately before the onset of the visual and auditory warnings, so that deceleration would reach ~0.10 g at approximately the same time as the visual and auditory warning onset. Peak deceleration from the haptic pulse was ~0.3g.

To appropriately activate the DVI, the WSU required vehicle kinematic data from which the threat assessment was performed. The OEM vehicle network provided data such as brake status and velocity to a Netway box. The Netway box, exclusively programmed by each of the OEMs, was used to translate OEM-specific controller area network (CAN) messages to a standardized CAN format compatible with the WSU.

A GPS system provided longitude/latitude positioning data to the WSU. This allowed the WSU to place the vehicle on a digital representation of the intersection called the Geometric Intersection Description (GID). GIDs were obtained from one of the three RSEs located at the signalized intersections. The RSEs provided GIDs for both stop-controlled and signalized intersections. Each GID was retained on the WSU unless a newer version was provided by the RSE.

In addition to the GIDs, the RSEs also sent differential GPS corrections (allowing the vehicle to accurately place itself on the GID) and signal phase and timing (SPaT) information. The messages were sent by a second WSU within the RSE. The SPaT message was supplied to the RSE by custom firmware installed on the traffic signal controllers, while a GPS base station provided the differential corrections.

**Vehicle DAS** - The vehicle DAS was used to record digital video and kinematic data from multiple sources, and was composed of hardware, software, and data storage components (Stone et al., in print). The DAS collected variables representing the information necessary to reconstruct a vehicle's intersection approach and the drivers' interaction with the CICAS-V. A short overview of the DAS is provided in this section.

The vehicle DAS hardware consisted of a main unit, a video system, front and rear radar, and a GPS unit. The main unit contained an Embedded Platform for Industrial Computing (EPIC) single-board computer, hard drive, CAN communication, battery backup system, and several VTTI-developed sensor modules. Four unobtrusive cameras installed in the passenger compartment captured the scene in and around the vehicle.

The DAS was attached directly to the OBE CAN which provided all of the CICAS-V variables. The DAS recorded the CICAS-V variables for use in system validation and driver performance analyses. Variables pertinent to the study included the velocity, distance to the stop bar, DVI status, signal phase and signal timing. Additional variables were also collected by the DAS from a network of sensors installed on the vehicle. Front and rear radar units provided the range and velocity of lead and following vehicles. A Crossbow™ inertial measurement unit provided three-axis acceleration and angular rate information.

Data were stored on a 120GB removable hard drive within the main unit. It was accessed and downloaded to a laptop over an Ethernet interface. The download interface included a system health-check component that ensured data integrity was maintained between drivers. This allowed quick transfer of data and indication of whether the participant received a warning without shutting down the system.

**Custom-built Navigation System** - In order to ensure that drivers could easily and reliably navigate the prescribed route, VTTI built a custom navigation system. The custom navigation system consisted of a laptop computer and a low cost Wide Area Augmentation System (WAAS)-enabled GPS antenna. The system played auditory instructions over a speaker in the front of the vehicle based on the current position of the subject along the route. The custom software solution allowed the researchers to record the instructions to play and to guarantee the timing of the instructions so as not to distract the driver while approaching an equipped intersection.

**Pseudo-Naturalistic Study Protocol**

Upon arriving at the Institute, participants were met by the greeter and asked to read an informed consent form. The form provided specific information about the study, including the procedures, risks involved, and measures for confidentiality. After agreeing to the study and signing the informed consent, a health screening questionnaire was administered to ensure that participants did not have any conditions that would impair their ability to safely operate the test vehicle. A Snellen vision test was conducted to ensure the participants' visual abilities were within Virginia legal limits of corrected to 20/40 or better. A color vision test was conducted using the Ishihara Test for Color Blindness, and a contrast sensitivity test was performed. The color vision test and the contrast sensitivity tests were recorded for possible future analyses but were not used for screening purposes. If it was found that participants were not in good health, or if vision results fell outside the acceptable limits, they would be excused from the study and paid for their participation time. Eligible participants were issued a short pre-drive questionnaire focusing on their driving experiences and habits.

The pseudo-naturalistic field test was conducted on a predetermined route in Blacksburg and Christiansburg, Virginia. The route was crafted to pass through many stop-controlled and signalized intersections while performing a variety of maneuvers (i.e., straight, left, and right turns). The route was approximately 36 miles long, and contained 13 intersections that were integrated into the CICAS-V. Three signalized and 10 stop-controlled intersections were chosen for evaluation.

The route led drivers through each equipped intersection multiple times and was designed with three goals in mind. First, to ensure the driving participants' comfort and minimize driving fatigue, the route had to be less than 2 hours in duration. Second, the route had to maximize the number of intersection crossings while retaining a feasible number of intersections (time constraints did not allow for a large number of intersections to be integrated into the CICAS-V). Finally, a variety of turn maneuvers were desirable in order to fully test the CICAS-V. For example, correct operation of the CICAS-V at signalized intersections often depends upon lane position information; therefore, various turn maneuvers at signalized intersections would indicate if the system was correctly mapping the lane to its signal indication. Also, a driver's intersection approach often has different trajectory characteristics if the driver is turning left, right, or straight through the intersection; accommodating these approach variations directly relates to algorithm evaluation. The turn maneuver summary table for the 13 intersections can be seen in Table 1. There were a total of 20 signal-controlled intersection crossings and 32 stop-controlled intersection crossings along the route.

**Table 1.**
**Summary of Turn Maneuvers for Pseudo-Naturalistic Study Experimental Method**

| 3 Signalized Intersections | | | | 10 Stop-Controlled Intersections | | | |
|---|---|---|---|---|---|---|---|
| **Permissive Left** | **Protected Left** | **Straight** | **Right** | **Left** | **Straight** | **Right** | **Total** |
| 2 | 5 | 11 | 2 | 12 | 6 | 14 | 52 |

After undergoing the initial paperwork process, participants were led outside where the experimenter introduced them to the test vehicle. Participants were given a brief tutorial on basic vehicle functions, including ignition procedures, seat movement, and the HVAC (heating, ventilation, and air conditioning) system. During the static pre-drive vehicle orientation, the different safety systems available in the experimental vehicle were briefly reviewed. The systems reviewed with the participants were the forward collision warning, backing aid, and the CICAS-V such that drivers were led to believe that various safety systems were being evaluated. The goal was to make the driver aware of the CICAS-V but not to emphasize it over the other available vehicle safety technologies.

During the route, participants received turn-by-turn directions from the custom-built GPS-based navigation system. The navigation system was audio-based and not an integrated vehicle system; therefore, in order to alleviate additional distractions, participants were instructed not to use the radio or CD player for the duration of the test drive. Emergency procedures were reviewed, including the location and proper use of a cellular telephone provided by VTTI. Participants were encouraged to call the experimenter at VTTI, from a stopped location, using a number taped to the phone if they encountered any problems (e.g., getting lost, failure of the navigation system, or mechanical problems with the vehicle). Once participants felt comfortable with the vehicle, they began the Pseudo-Naturalistic Study without any experimenter in the vehicle.

When participants returned, a laptop running specialized software was attached to the trunk-mounted DAS. While the experimenter downloaded the data, the interface indicated the number of warnings that were issued and the number of intersections that were crossed. This interface was used to determine which of the questionnaires was administered, based on whether a warning was issued. In addition, the number of equipped intersection crossings was used to determine the extent to which the driver experienced the entire test route. Since an experimenter was not present in the vehicle, it was foreseeable that some drivers might not follow the prescribed route or would not correctly understand the navigation instructions. Therefore, to motivate drivers to stay on route, a bonus was provided for drivers who crossed more than 40 equipped intersections.

At the same time, the greeter met the participants and led them indoors to a private office. Drivers then completed one of two post-drive questionnaires depending on whether they did or did not receive a warning. The questionnaires assessed what aspects of the CICAS-V system the drivers noticed and what they thought of the system.

Upon completion of the post-drive questionnaire, participants were paid, thanked for their time, and dismissed. The route took approximately 2 hours to complete, and with pre- and post-drive procedures, total participation time was 2 hours 45 minutes.

An important note for the Pseudo-Naturalistic Study protocol is that not every participant in the study experienced the same warning algorithms. As stated previously, one of the goals of the study was to iteratively refine the warning algorithm. In other words, researchers conducted initial data reviews to determine the success of the warning algorithms, and make changes based on the driving outcomes. This aspect of the study, including the breakdown of subjects receiving each algorithm, is discussed in detail in the Results and Discussion section.

**Validation and Analysis Techniques**

Recall that the primary purpose of the study was to determine how well the CICAS-V operated in order to determine if the system was mature enough for an FOT. To determine the validity of a violation warning, several variables in addition to the video were viewed by the data reduction staff. These were:

- DVI Status: The DVI was disabled because the vehicle was not within range of an intersection, or it was within range of an intersection and providing the blue "intersection ahead" icon, or it was within range of an intersection and providing a violation warning.
- Current Approach Phase: Red, Yellow, or Green
- Brake Status: The driver was either pressing the brake or not pressing the brake.
- Distance to Stop Bar (m): Distance from the front of the vehicle to the stop bar. This was used together with "vehicle speed" to determine if the algorithm was warning correctly.
- Improved Distance to Stop Bar (m): Distance to stop bar with missing points filled in using GPS. The raw Distance to Stop Bar provided by the WSU would drop out whenever the vehicle was not placed on the GID. The Enhanced Distance to Stop Bar continued to provide data during those drop outs.
- Intersection ID: The identification number that was assigned to each CICAS-V intersection and incorporated into the GID.
- Longitudinal Acceleration (g): Used to determine whether or not the brake pulse activated appropriately.
- On GID: A binary indication of whether the vehicle is map-matched to the GID. It was used to determine when the vehicle was not map-matched within the warning region.
- Present Lane: As labeled and identified in the GID. Associated with the signal phase and video to ensure that the system was identifying the correct lane position and warning accordingly.
- SPaT Counter: A counter that increments when the OBE is receiving messages from the RSE. It was used to determine when SPaT messages were not received within the warning region.
- Vehicle Speed (m/s): Used with "distance to stop bar" to determine if the algorithm was warning correctly.

The primary goal of data reduction was to validate CICAS-V warnings that were automatically identified in the parametric data. Data reductionists determined if the CICAS-V warning was appropriate by reviewing the video. For the signalized intersections, data reductionists examined the intersection signal phase and timing relative to the vehicle proximity to the stop bar. If the signal phase was red and the vehicle was over the stop bar, the warning was deemed appropriate. For the stop-controlled intersections, data reductionists verified that the warning was provided at a stop-controlled intersection and prior to the vehicle crossing the stop bar.

The Data Analysis and Reduction Tool (DART) was used to validate events. DART is a software package developed at VTTI that provides a user interface for the viewing and reducing of digital data. It contains user-configurable video and graphical interfaces, and allows users to simultaneously view synchronized video and graphical data streams frame by frame.

## RESULTS AND DISCUSSION

Ninety-three drivers participated in the Pseudo-Naturalistic Study. System failures (that will be discussed later in the paper) caused data to be retained for 87 drivers; these data were utilized to complete the analyses for the Pseudo-Naturalistic Study, as summarized in Table 2.

**Table 2.**
**Distribution of Drivers by Age and Gender who had Data Analyzed in the Pseudo-Naturalistic Study Analyses**

| Age Group | Gender | | Total |
|---|---|---|---|
| | Male | Female | |
| **18-30** | 17 | 15 | 32 |
| **35-50** | 10 | 14 | 24 |
| **55+** | 15 | 16 | 31 |
| **Total** | 41 | 45 | 87 |

Recall that one of the goals of the study was to iteratively refine the warning algorithm. In other words, researchers conducted initial data reviews to determine the success of the warning algorithms and make changes based on the driving outcomes. Because drivers approach stop-controlled intersections differently than they approach signalized intersections, two algorithms were used. The algorithms, the process for evaluation, and the criteria for determining success are discussed in the following sections.

**Stop-Controlled Algorithm 1 Results** - The initial stop-controlled intersection warning algorithm incorporated into the CICAS-V was derived directly from the results of a previous CICAS-V study, Neale et al. (in print). Over 160 algorithms were analyzed during the course of that effort. The performance of each potential algorithm was based on its effectiveness in predicting a pending violation while minimizing false detections based on naturalistic intersection approach data. In addition, other measures, such as the location at which a violation warning would be provided, likelihood of annoyance, algorithm complexity, and data requirements, were also considered.

Fifteen drivers experienced Stop-Controlled Algorithm 1, resulting in a total of 493 stop-controlled intersection crossings with 50 CICAS-V warnings being initiated. (Note that there were 32 stop-controlled intersection crossings on the route. When multiplied by the 15 drivers experiencing Stop-Controlled Algorithm 1, one would expect a total of 480 crossings. However, a few drivers made wrong turns along the route and actually crossed the intersections more often than was planned.) Table 3 illustrates the distribution of drivers, by age and gender, which experienced Stop-Controlled Algorithm 1.

**Table 3.**
**Distribution of Drivers by Age and Gender who Experienced Stop-Controlled Algorithm 1***

| Age Group | Gender | | Total |
|---|---|---|---|
| | Male | Female | |
| **18-30** | 2 | 1 | 3 |
| **35-50** | 1 | 4 | 5 |
| **55+** | 4 | 3 | 7 |
| **Total** | 7 | 8 | 15 |

*Note: These drivers are a portion of the total number of drivers who participated in the Pseudo-Naturalistic Study.

Since the data were downloaded after each drive, the number of warnings was immediately displayed on the vehicle DAS, which provided quick general feedback about alert frequency. When the driver received at least one warning, researchers reviewed the parametric and video data in detail to determine the prevalent conditions of each warning. A review of the warnings indicated that the subset of drivers who experienced alerts received them at five stop-controlled intersections. After reviewing the intersections' geometry, it was noted that the alerts were occurring on intersection approaches that had a 3.8 to 7% uphill grade.

Stop-Controlled Algorithm 1 considered brake status when determining whether drivers should receive a violation alert. That is, if a driver was pressing the brake, it was assumed the driver was attentive to the intersection and the alert was suppressed. On uphill grades, drivers tended to press the brake later in their approach, using gravity to slow the vehicle. Since the algorithms were developed on flat intersection approaches, the later braking caused the warning to activate more often than was expected.

A review of the video and questionnaire data (discussed later) indicated that, although the drivers always came to a safe stop, they tended to become either annoyed or, possibly, entertained by repeated warnings. Based on these results, the decision was made to change the warning algorithm for stop-controlled intersections to one that did not rely on brake status to determine when a warning should be initiated. After reviewing the possible algorithms discussed in Neale et al. (in print), a new algorithm (Stop-Controlled Algorithm 2) was selected and integrated into the OBE.

The post-drive questionnaire was completed by the 13 drivers who received the total 49 valid warnings at stop-controlled intersections. Data show that drivers found the alerts useful, effective at communicating a possible violation, and attention getting. There were also several potential negative trends in responses. More drivers responded that, when receiving a violation warning, they tended to brake without checking for following traffic. Also, drivers tended to find the alert annoying when it was deemed unnecessary. This response is not surprising, and, in part, motivated the change to Stop-Controlled Algorithm 2. Three drivers admitted to intentionally trying to activate the warning system and three drivers said they would have turned the system off if they could. It is interesting to note that both aspects of the visual DVI, the blue "intersection ahead" icon and red flashing visual alert, were viewed less favorably than the speech alert and brake pulse warning. Several drivers noted, in the open-ended comment section, that they did not notice the visual icons. Suggested potential improvement to the visual DVI included a more conspicuous visual display that was a little larger and placed closer to the driver.

**Stop-Controlled Algorithm 2 Results** - Subtask 3.2 predicted that Stop-Controlled Algorithm 2 would correctly warn 60% of the violators and incorrectly warn less than 5% of the compliant drivers. A total of 72 drivers completed the Pseudo-Naturalistic Study protocol using the revised warning algorithm (Table 4). This resulted in a total of 2,125 valid intersection crossings at stop-controlled intersections with a total of three warnings issued. (Again, recall that there were 32 stop-controlled intersection crossings. When multiplied by the 72 drivers, one would expect a total of 2,304 crossings. However, as will be discussed in the Evaluation of the Study Systems section, data were sometimes lost due to system deficiencies.)

**Table 4.**
**Distribution of Drivers by Age and Gender who Experienced Stop-Controlled Algorithm 2***

| Age Group | Gender | | Total |
|---|---|---|---|
| | Male | Female | |
| **18-30** | 15 | 14 | 29 |
| **35-50** | 9 | 10 | 19 |
| **55+** | 11 | 13 | 24 |
| **Total** | 35 | 37 | 72 |

*Note: These drivers are a portion of the total number of drivers who participated in the Pseudo-Naturalistic Study.

All three warnings occurred at the same intersection while making the same straight-crossing maneuver. The intersection is in the middle of a straight road with a stop sign that is partially occluded at longer distances. The violation warnings were provided to three different drivers: a younger male, a middle-aged male, and an older male. In all three cases, they did not show indications of intending to stop prior to the warning, yet stopped before entering the intersection box after the warning was issued. The drivers' peak decelerations ranged from 0.46 g to 0.6 g and the average decelerations ranged from 0.33 g to 0.41 g.

The post-drive questionnaire results from drivers who experienced Stop-Controlled Algorithm 1 can be compared to those provided by the three drivers who each experienced a single violation warning while driving with Stop-Controlled Algorithm 2. These three drivers were issued a warning at the same occluded intersection. The subjective responses from these three drivers were more favorable than those provided by drivers who experienced Stop-Controlled Algorithm 1. This is an expected outcome, since one would expect that drivers who experienced the CICAS-V in the manner it was intended to operate (rare warnings issued only when needed by the driver) would find the system more agreeable. Overall, drivers were satisfied with the system and recognized that they were in danger of violating the stop sign when they received the warning.

**Signalized Intersection Algorithm Results**

The signal-controlled intersection warning algorithm incorporated into the CICAS-V was also developed during the previous CICAS-V effort report in Neale et al. (in print). The Signalized Intersection Algorithm was predicted to correctly warn 83% of the violators and incorrectly warn less than 5% of the compliant drivers. As will be discussed, the warning was deemed successful throughout data collection and was not changed. Therefore, the CICAS-V utilized the same signalized warning timing for all drivers who participated in the Pseudo-Naturalistic Study. A total of 87 drivers completed the pseudo-naturalistic protocol, as summarized in Table 5. This resulted in a total of 1,455 valid intersection crossings at signalized intersections.

Recall that there were 20 signal-controlled intersection crossings that occurred through the three instrumented signalized intersections. When multiplied by the 87 drivers, one would expect a total of 1,740 crossings. However, as will be discussed in the Evaluation of the Study Systems section, data were sometimes lost due to system deficiencies.

**Table 5.**
**Distribution of Drivers by Age and Gender who Experienced Signalized-Warning Algorithm during the Pseudo-Naturalistic Study***

| Age Group | Gender | | Total |
|---|---|---|---|
| | Male | Female | |
| **18-30** | 17 | 15 | 32 |
| **35-50** | 10 | 14 | 24 |
| **55+** | 15 | 16 | 31 |
| **Total** | 41 | 45 | 87 |

*Note that these are all drivers who participated in the Pseudo-Naturalistic Study since the algorithm did not change.

A total of seven violation warnings occurred at signalized intersections: one valid warning, two invalid warnings due to an emergency vehicle signal preemption, and four invalid warnings due to an incorrect GID for the intersection.

For the valid warning, a middle-aged male approached a signalized intersection to make a straight-crossing maneuver. He was in the right-most straight through-lane following a vehicle with about 1-second headway. The signal became visible in the video at 53m (173 ft) and is in the yellow state. The driver does not show any indication of intending to brake until after the pre-warning process (a 500 ms process to initialize the warning) had started. Three-hundred ms later, the driver begins to brake. The pre-warning process finished and a warning is issued 200 ms after the braking began. The driver brakes safely to a stop before crossing the stop bar. Although it cannot be determined with certainty, the driver's braking prior to the warning likely indicates intent to stop. The driver did not show any visible expression in response to the warning. If the driver had not stopped, it appears a violation would have occurred, based on the location of the lead vehicle, which crosses over the stop bar as the signal turned red.

Two similar invalid warnings occurred when an emergency vehicle preempted the traffic signal. In both cases, the drivers were approaching a signalized intersection within a few minutes of the emergency vehicle. When the emergency vehicle approached the intersection, the traffic controller switched to a priority mode, which guarantees a green phase for the emergency vehicle. Unfortunately, the specialized firmware installed in the traffic controllers did not update the RSE with the correct SPaT messages when the signal was in the priority mode. As a result, the CICAS-V interpreted the signal phase as red when, in actuality, the preemption had caused the signal to turn green. This resulted in CICAS-V warnings issued on a green phase. One of the drivers handled the false warning in a calm manner without making any abrupt driving maneuvers. The second driver appeared startled and initially slowed the vehicle in response to the alert. The driver then made a quick assessment of the situation and chose to proceed through the intersection. Notably, a following vehicle did have to slow in response to the test vehicle. The signal priority addressable system issue is discussed further in the Evaluation of the Study Systems section.

Finally, four invalid warnings occurred due to an incorrect GID for one of the signalized intersections. The faulty GID incorrectly labeled the left-most through lane as the left turn lane, and associated the through lane with the dedicated left-turn signal head. The problem occurred when the drivers were making a straight-crossing maneuver in the left-most through lane, which had a green-phased light; the adjacent left-turn lane had a red-phased light. The CICAS-V would note the red-phase for the left-turn lane, and warn the driver who was actually in the through lane with a green-phase.

The problem of the incorrect GID was identified by the research team the first time that a false alert was issued. However, since the driver responded calmly to the false alert and proceeded through the intersection appropriately, the incorrect GID was left in place. This allowed the team to learn more about how drivers respond when receiving a false alert during a green phase. The second and third time this occurred, those drivers also responded in a calm manner, assessed the situation quickly, and proceeded through the intersection. The final driver, however, was very startled by the warning on a green phase, and responded with abrupt braking that, under some conditions, had the potential to result in a rear-end collision with the following vehicle. Of particular importance, a following vehicle both applied the brakes and steered around the test vehicle in order to avoid a collision. Following this event, the correct GID was loaded onto the RSE. This issue is discussed further in the Evaluation of the Study Systems section.

The post-drive questionnaire was completed by the six drivers who experienced an invalid signalized violation warning while driving. One of these six drivers also received one valid signalized intersection violation warning. Overall, drivers thought the system was effective and did not rate the system as distracting or annoying. This is likely due to the fact that, even though the alerts were invalid, the alert frequency was considerably lower than with Stop-Controlled Algorithm 1. Also consistent with responses by drivers who received valid alerts, the red flashing visual alert and the "intersection ahead" icon were viewed less favorably than the speech and brake alerts.

**Questionnaire Results from Drivers Who Did Not Experience a Violation Warning -** Recall that drivers who completed the study without receiving a violation warning also completed a questionnaire. For these drivers, the only exposure to the CICAS-V would have been the opportunity to notice the blue "intersection ahead" icon at equipped intersections. Therefore, this questionnaire contained few questions, most of which asked the driver to rate their experiences with the "intersection ahead" display. The results are interesting in that there is a trend indicating that the drivers did not find the blue "intersection ahead" icon annoying or distracting; however, these drivers also felt that the visual-only

DVI was ineffective in communicating the intended information and not easily detected. Drivers often did not complete the questionnaire, presumably because they did not notice the blue icon. These results are consistent with the other questionnaire results that indicate that drivers often did not notice the blue "intersection ahead" display. Interestingly, many drivers took the time to provide feedback in the final open question on the questionnaire. Overall, drivers expressed a desire to have the display be more conspicuous.

**Evaluation of the Study Systems**

One goal of the study was to evaluate the CICAS-V and DAS hardware and software performance on live roads in order to demonstrate FOT readiness. However, it should be noted that the CICAS-V software tested during the field test was not the final software release. Version 1.11 of the software was implementable for this field test at the time of testing; however, the final release was Version 1.15. There were several improvements to the software during the releases after 1.11 that would have likely improved the results presented in this section. In particular, as will be discussed shortly, improvements made in the intersection selection method and the wireless protocol updates may have improved the system performance, as shown by tests performed in other CICAS-V tasks (Maile et al., in print-b, in print-a).

Another important note is that the DAS was not equipped with an independent set of sensors to verify these data. As a result, these analyses are somewhat limited in that they assume that the data provided by the WSUs are accurate.

The CICAS-V hardware and software were evaluated using two metrics; the system log and the DVI status variable. The system log was maintained by the experimenters. It consisted of a list of hardware and software issues that were encountered during the study. Most of the problems identified from the system log were addressed with upgrades to the CICAS-V application software or were not problems with the CICAS-V system itself. The predominant log entry indicated a Netway box failure. When the Netway failed, the WSU did not receive vehicle network information (e.g., speed). Without this information, the system was unable to perform the CICAS-V functions. Portions of several drives, and in some cases, entire drivers were lost due to this malfunction. Approximately 5% of data were lost due to this deficiency.

The DVI status variable was used to identify how often the CICAS-V was fully capable of providing a warning. Using the blue "intersection ahead" icon as the indicator of the range of the vehicle, it was identified that the CICAS-V was enabled 96% of the time at either stop-controlled or signalized intersections. When the system was disabled, over half of the periods were longer than 1 second. From these results, it appears that most of these periods have the potential to result in a late warning if the driver happens to violate while the system is disabled, and the impact on the CICAS-V effectiveness may be substantial, potentially negating the CICAS-V safety benefit.

The hardware and software of the vehicle DAS were evaluated. The vehicle DAS hardware and software showed less than a 1% data loss.

## RECOMMENDATIONS AND STUDY LIMITATIONS

This study was a pilot test to perform the first on-road naïve-driver system-level test of the CICAS-V. The following sections describe the implications that may be drawn.

**The CICAS-V System is FOT Ready**

The on-road data collection indicated that the CICAS-V functions reliably and as intended for the purpose of conducting an FOT. The issues that were noted with the system during data collection have already been largely resolved with CICAS-V application software upgrades. The problems that are outstanding at the time of writing this paper are not problems with the CICAS-V itself, but relate to just this initial implementation. First, the invalid warnings that occurred when an emergency vehicle preempted the signal, which caused the RSE to report incorrect phase information, are being addressed by the signal controller company. The occasional failure of the Netway box during data collection is not an issue of the CICAS-V per se; however, it is an issue that would need further attention in order to minimize data loss during an FOT. Approximately 5% of data were lost due to this deficiency. For the FOT, it is likely that the WSU software would be specialized for each vehicle platform, making the Netway box unnecessary.

**CICAS-V Algorithms are FOT Ready**

The study successfully tested two algorithms for stop-controlled intersections and one algorithm for signalized intersections. Although Stop-Controlled Algorithm 1 was not deemed successful, its successor, Stop-Controlled Algorithm 2, successfully warned three different drivers of an occluded intersection. Signalized Intersection Algorithm 1 provided a valid and timely warning to a driver approaching a light through a phase change.

**The Vehicle DAS is FOT Ready**

The Vehicle DAS performed well during the study. Although there was a hard drive malfunction during the course of the study, very little data were lost (2 hours out of 191 hours total) due to Vehicle DAS equipment failures. It is recommended that variables that were not useful for the pilot be eliminated from collection to save storage space and simplify the resulting database.

**Pilot Study Protocols are FOT Ready**

The protocols, pre-drive questionnaires, and post-drive questionnaires worked well for the pilot study and can be implemented during an FOT.

**The CICAS-V Appears to Provide a Benefit to the Driver**

Every driver who was provided with a valid violation warning throughout data collection came to a stop before the intersection box. The valid violation warnings provided from the best performing algorithms, Stop-Controlled Algorithm 2 and the Signalized Intersection Algorithm, are of particular interest since the scenarios mimic those for which the CICAS-V was designed. Those scenarios are an occluded stop-controlled intersection that drivers had trouble detecting, and a signalized intersection with lead traffic going into a phase change. Of course, the results from this study alone cannot provide an accurate cost/benefit trade off, but the results from this study indicate a potential benefit of the system.

**Drivers like the CICAS-V**

Subjective data on post-test questionnaires indicate that drivers generally like the CICAS-V. A common critique of the system was the conspicuity of the visual display. Nonetheless, this is a minor critique considering that: 1) the visual display was not designed into the original dash configuration and was added; 2) drivers had little time with the vehicle (2 to 3 hours) to become accustomed to the display; 3) the speech and brake pulse modalities are very effective; and 4) for the purposes of conducting an FOT, the visual display can be viewed as a secondary indicator to the speech and brake pulse warning modes and could be modified to improve conspicuity.

**Limitations of the Study**

One shortcoming of the research is that data collection concluded without benefit of testing the final version of the CICAS-V application. As stated, the study was conducted using Version 1.11 of the software. By the time data collection had ended and the experimenters had given feedback to the CICAS-V developers, Version 1.15 had been developed, reflecting four software upgrades and several incorporated system refinements. Therefore, it is recommended that a small study be conducted prior to an FOT to test the upgraded software.

Also, this study was conducted in the small metropolitan region of Blacksburg, Virginia. In this area, the GPS coverage was adequate for testing the system, the state Department of Transportation was very supportive, and the proximity to data collectors was ideal. Alternative locations are likely to provide different and, likely, additional challenges relative to those that were met by the research staff. As such, the trade-offs of alternative locations would need to be carefully considered prior to selecting the final FOT site.

## REFERENCES

[1] Maile, M., Ahmed-Zaid, F., Basnyake, C., Caminiti, L., Kass, S., Losh, M., Lundberg, J., Masselink, D., McGlohon, E., Mudalige, P., Pall C., Peredo, M., Popovic, Z, Stinnett, J., and VanSickle, S. (In Print-a). Cooperative Intersection Collision Avoidance System Limited to Stop Sign and Traffic Signal Violations (CICAS-V) Task 11 Final Report: Objective Tests. Washington, DC: National Highway Traffic Safety Administration.

[2] Maile, M., Ahmed-Zaid, F., Basnyake, C., Caminiti, L., Kass, S., Losh, M., Lundberg, J., Masselink, D., McGlohon, E., Mudalige, P., Pall C., Peredo, M., Stinnett, J., and VanSickle, S. (In Print-b). Task 10 Final Report: Integration of Subsystems, Building of Prototype Vehicles and Outfitting of Intersections. (Cooperative Agreement No. DTFH61-01-X-00014). Washington, DC: National Highway Traffic Safety Administration.

[3] Maile, M., Neale, V., Ahmed-Zaid, F., Basnyake, C., Caminiti, L., Doerzaph, Z., Kass, S., Kiefer, R., Losh, M., Lundberg, J., Masselink, D., McGlohon, E., Mudalige, P., Pall C., Peredo, M., Perez, M., Popovic, Z, Stinnett, J., Sudweeks, J., VanSickle, S., and Kiger, S. (In Print-c). Cooperative Intersection Collision

Avoidance System Limited to Stop Sign and Traffic Signal Violations (CICAS-V) Phase I Final Report. Washington, DC: National Highway Traffic Safety Administration.

[4] Najm, W.G., Smith, J.D., & Yanagisawa, M. (2007). Pre-Crash Scenario Typology for Crash Avoidance Research (Report No. DOT HS 810 767). Washington, D.C.: National Highway Traffic Safety Administration.

[5] National Highway Traffic Safety Administration. (2006). Traffic Safety Facts – 2004 (Report No. DOT HS 809 919). Washington, D.C.: National Highway Traffic Safety Administration.

[6] Neale, V. L., Doerzaph, Z. R., Perez, M. A., Sudweeks, J., Kiefer, R., and Maile, M. A. (In Print). Cooperative Intersection Collision Avoidance System Limited to Stop Sign and Traffic Signal Violations (CICAS-V) Task 3 Final Report: Human Factors Research. (Cooperative Agreement No. DTFH61-01-X-00014). Washington, DC: National Highway Traffic Safety Administration.

[7] Stone, S., Neale, V. L., Wiegand, K., Doerzaph, Z. R. and Maile, M. (In Print). Cooperative Intersection Collision Avoidance System Limited to Stop Sign and Traffic Signal Violations (CICAS-V) Task 12 Final Report: Infrastructure and Vehicle DAS Functional Designs. (Cooperative Agreement No. DTFH61-01-X-00014). Washington, DC: National Highway Traffic Safety Administration.